

6.0 MODEL DESIGN

Model design involves selecting the code, size of model cells, and layers used to represent the aquifer. Models represent approximations and simplifications of a natural system. Assumptions and compromises due to the conceptual model, objectives, input data, software capabilities, and schedule and budget for developing a model influence the results, accuracy, and applicability of a model. Different combinations of input data can result in different model predictions. Model design and calibration are attempts at constraining possible simulation results. We designed this model to agree as much as possible with our conceptual model of the occurrence and movement of groundwater in the central Carrizo–Wilcox aquifer.

6.1 Code and Processor

The choice of code is necessary to ensure that important processes, including recharge, interaction of groundwater and surface water, groundwater ET, pumping at wells, and boundary fluxes in the aquifer, are modeled appropriately. This study used MODFLOW-96 (Harbaugh and McDonald, 1996) to solve the flow equation according to the finite-difference method (Anderson and Woessner, 1992). MODFLOW is a widely tested and used groundwater-modeling software that includes modules needed for simulating the hydrologic processes in the aquifer. Processing MODFLOW (PMWIN version 5.3.0; Chiang and Kinzelbach, 2001) was used as the modeling interface to help load and package data into the formats needed for running simulations in MODFLOW and for looking at simulation

results. We developed and ran the model on a Dell Optiplex GX400 with a 1.8 GHz Pentium 4 Processor and 1 GB RAM running Windows 2000.

6.2 Layers and Grid

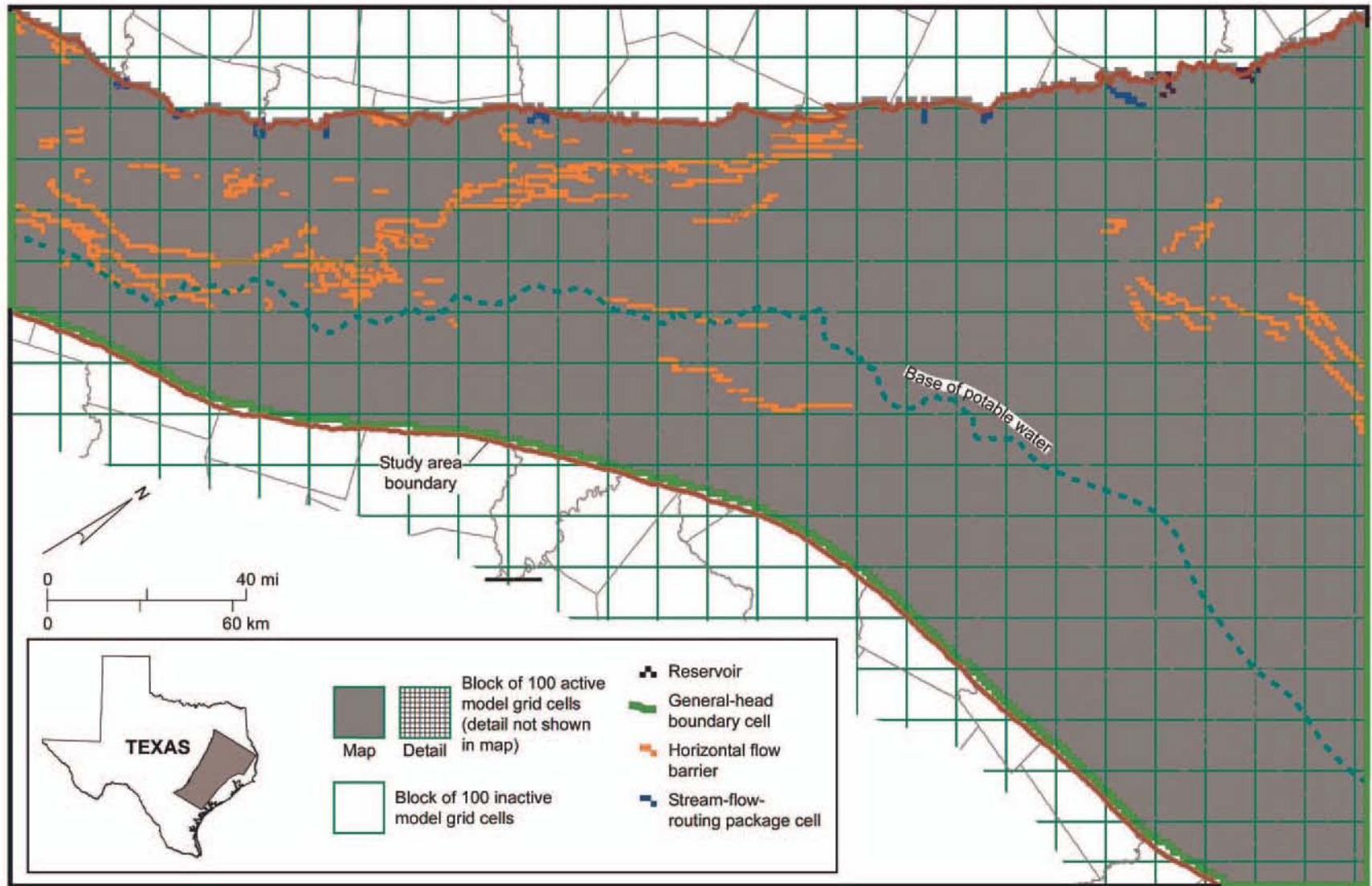
The lateral extent of the model roughly corresponds to natural hydrologic boundaries on the southwest, west, and southeast: (1) updip limit of the outcrop of host formations, (2) base or downdip limit of freshwater, and (3) presumed groundwater flow paths to the south. The southwestern boundary lies near the San Antonio River (fig. 2). The northwestern boundary is at the limit of the outcrop of the formations that make up the aquifer. The southeastern boundary coincides with the Wilcox Growth Fault Zone that roughly marks the updip limit of geopressed conditions in the aquifer (fig. 14). The northeast boundary of the study area runs from the aquifer outcrop in Van Zandt County, across part of the East Texas Basin, part of the Sabine Uplift, and then continues into the deep part of the Carrizo–Wilcox aquifer. We set an arbitrary boundary along this line. Groundwater flow paths in the vicinity of the lateral boundary on the northeastern side of the model have not remained constant during the past 20 to 50 yr owing to pumping in the vicinity of Jacksonville, Lufkin, Tyler, and other cities. Use of the northern Carrizo–Wilcox model may provide more representative results in this overlap area (fig. 3). The southwestern boundary of the northern Carrizo–Wilcox model is sufficiently distant from the pumping centers in Jacksonville, Lufkin, and Tyler that results are not affected by the boundary condition.

We defined six model layers. The bottom four layers represent the main parts of the Carrizo–Wilcox aquifer in the study area. Groundwater in the Hooper, Simsboro, Calvert Bluff, and Carrizo Formations is modeled in layers 6, 5, 4, and 3, respectively

(figs. 10, 54 through 57). In MODFLOW layers are numbered from top to bottom.

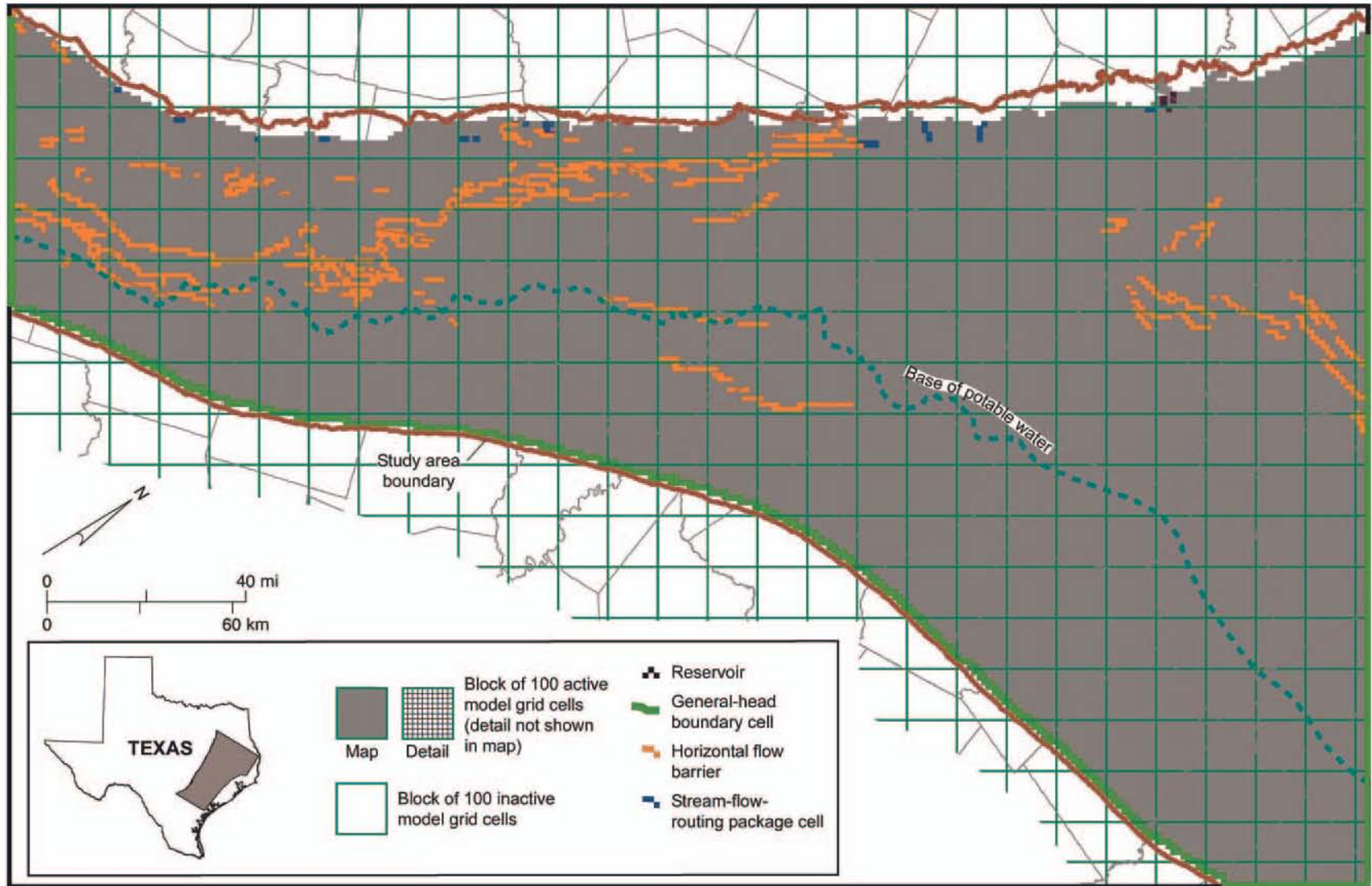
Layer 6 is the basal unit of the model; we assumed that no flow of groundwater occurs between the Hooper Formation and the underlying Midway Formation. Layer 2 represents the Reklaw Formation (fig. 58), which functions as a confining layer or aquitard between the Carrizo–Wilcox aquifer and the overlying Queen City aquifer. Layer 2 in the model has the role of applying a boundary condition across the top of the model. The uppermost layer 1 represents alluvium in the valleys of the Colorado, Brazos, and Trinity Rivers (fig. 59). Some of the active cells assigned in layers 2 through 5 are beneath the alluvium of layer 1 but above the uppermost bedrock layer. Using MODFLOW, we found it necessary to create additional active cells in these layers to allow a connection between the alluvium modeled in layer 1 and the underlying bedrock layer. These additional cells are apparent in figures 55 through 58 as narrow northwestward extensions of the active cells of model layers.

The model grid consists of 273 columns and 177 rows of square model cells that measure 1 mi on a side. This grid-cell size is considered small enough to reflect the density of data for building and calibrating the model, while large enough for the model to be manageable. Uniform grid-cell dimensions simplify the use of digital mapping and spreadsheets to input data into the model. There are 289,926 cells in the 273-column × 177-row × 6-layer model. Only 120,477, or about 42 percent, of these are active cells representing the aquifer at which calculations are made. Layer 1 has only 383 active cells, whereas layers 2 through 6 have more than 21,000 active cells each (21,857 in layer 2, 22,602 in layer 3, 24,560 in layer 4, 25,067 in layer 5, and 26,008 in layer 6). Cell thickness represents the thickness of model layers (for example, figs. 23 through 26).



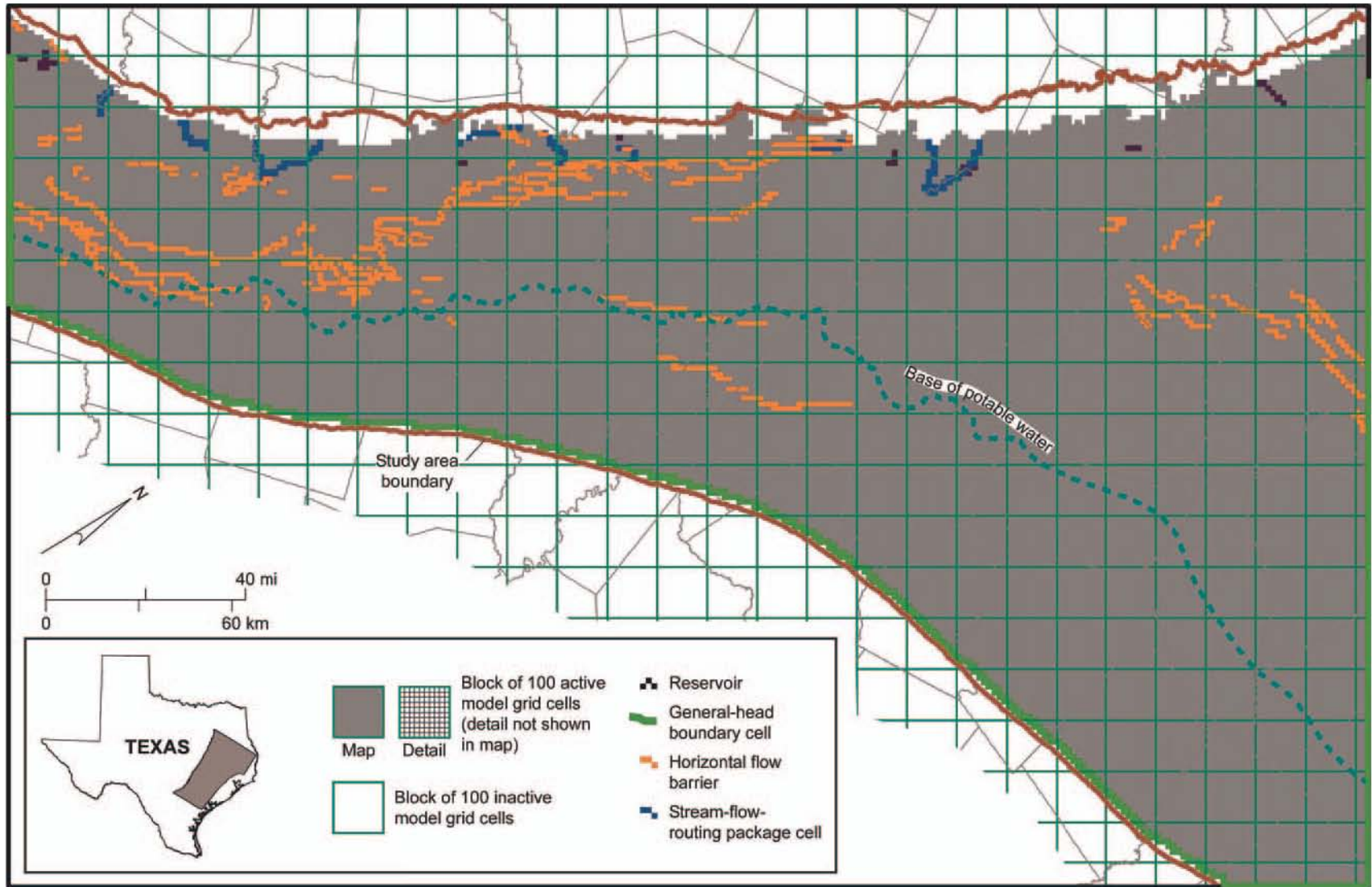
QAd2043c

Figure 54. Location of active cells in model layer 6, representing groundwater in the Hooper Formation, and the position of boundary cells.



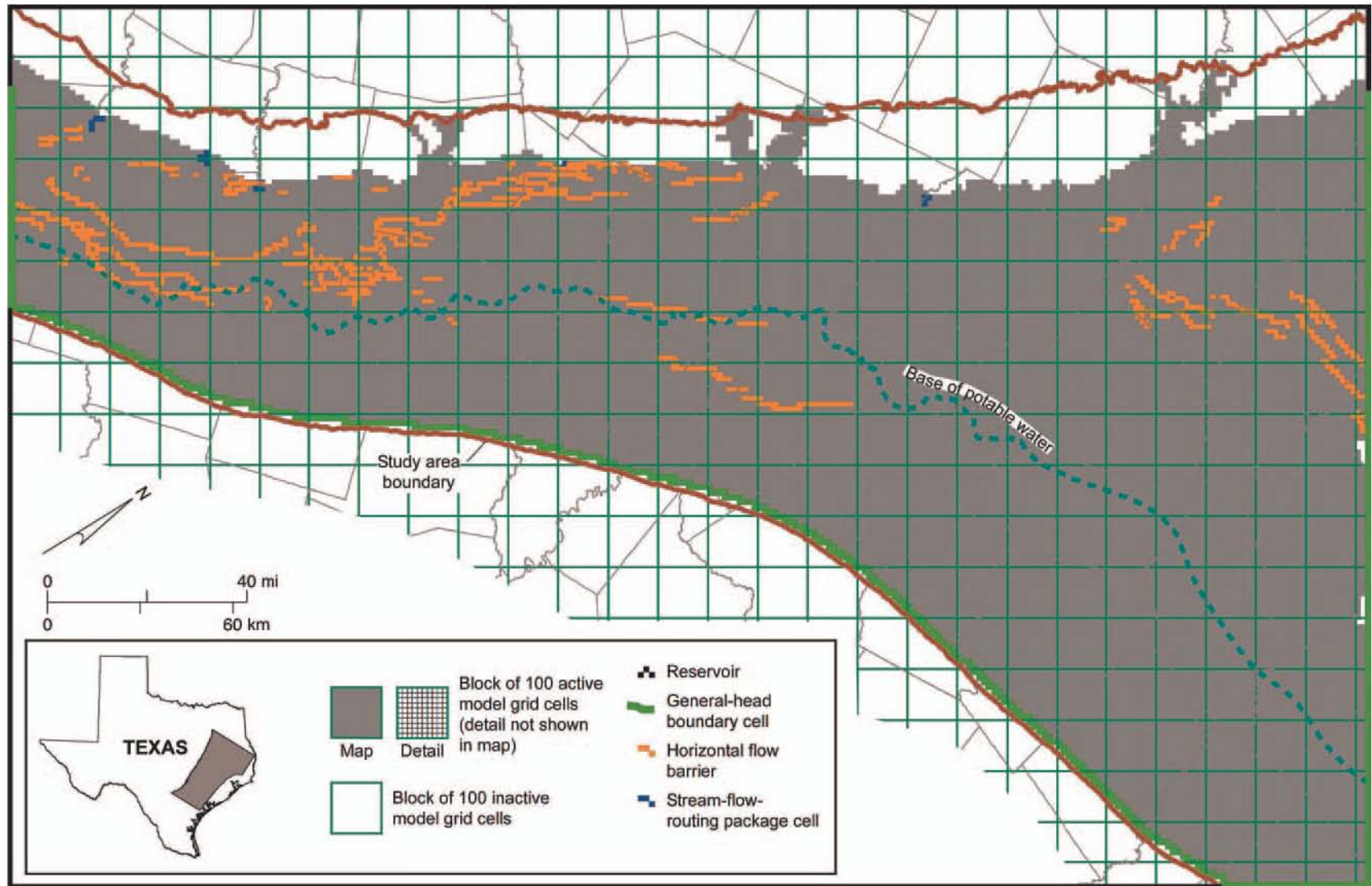
QAd2044c

Figure 55. Location of active cells in model layer 5, representing groundwater in the Simsboro Formation, and the position of boundary cells.



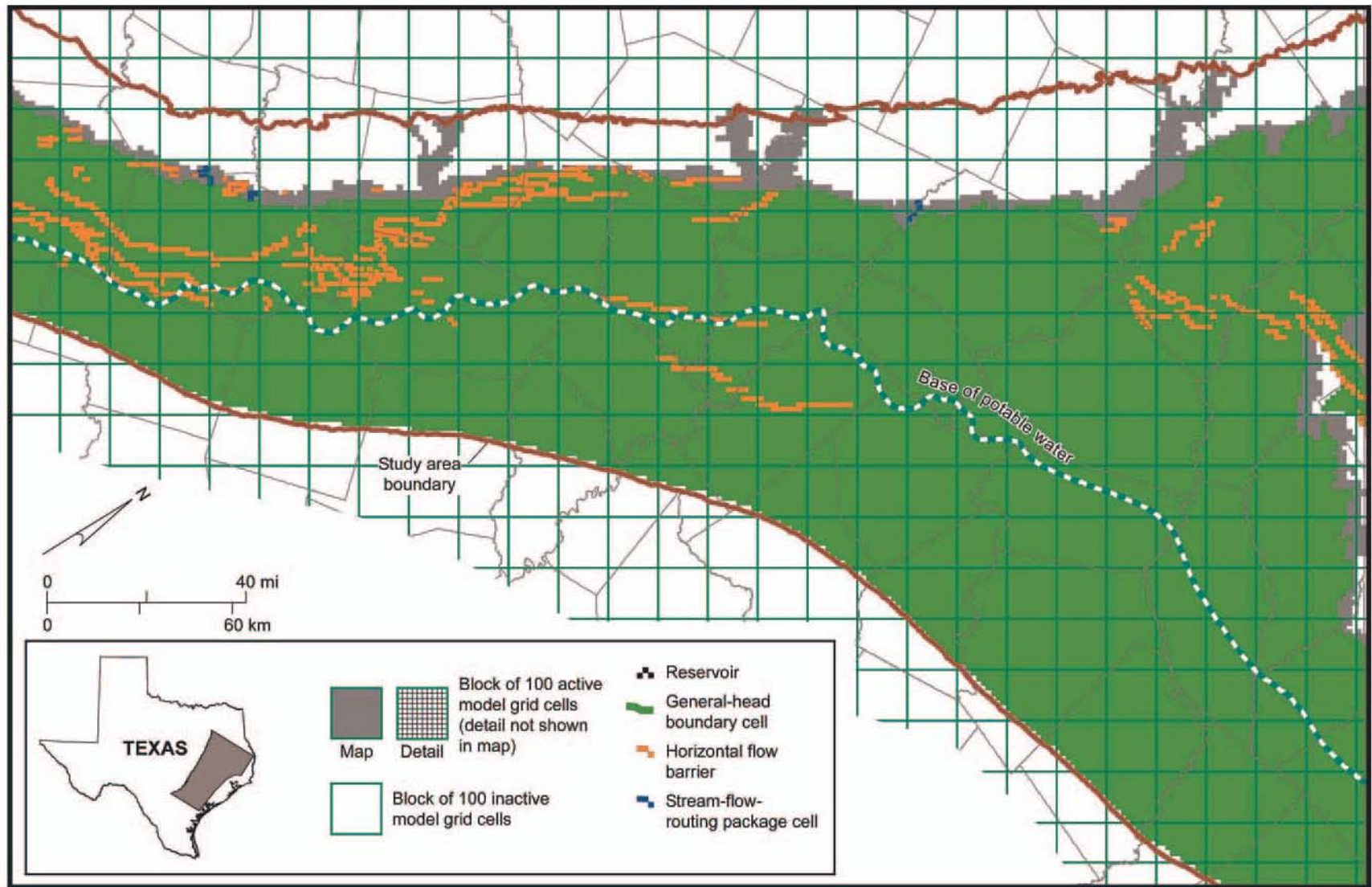
QAd2041c

Figure 56. Location of active cells in model layer 4, representing the Calvert Bluff Formation, and the position of boundary cells.



QAd2042c

Figure 57. Location of active cells in model layer 3, representing the Carrizo Formation, and the position of boundary cells.



QAd2039c

Figure 58. Location of active cells in model layer 2, representing the Reklaw Formation, and the position of boundary cells.

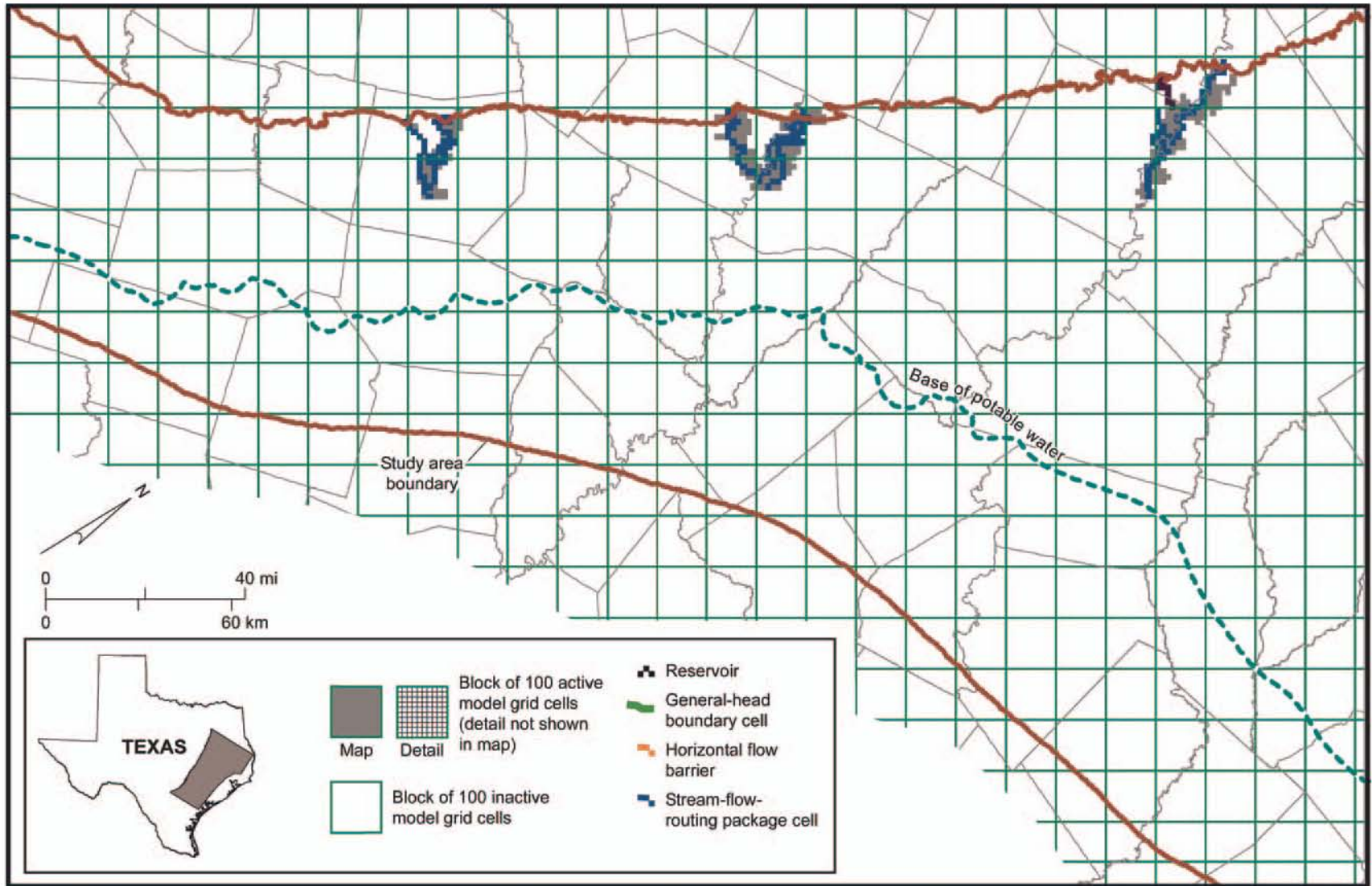


Figure 59. Location of active cells in model layer 1, representing alluvium in the Colorado, Brazos, and Trinity River systems, and the position of boundary cells.

QAd2040c

Rows of the model were aligned parallel to the strike of the Wilcox outcrop on the northwestern side of the study area. The model grid origin (X_0 , Y_0) is located at GAM coordinates of 5,382,716 ft Easting and 18,977,220 ft Northing with the x axis rotated 58° positive or counterclockwise. The geographic projection parameters for the model grid and hydrogeologic data are given in table 9.

6.3 Boundary Conditions

Boundary conditions account for movement of water into and out of the model domain and represent the natural flow and pumping in the aquifer. Boundary conditions for the Carrizo–Wilcox aquifer are applied in the model using standard modules in MODFLOW. Boundary values were applied to all six faces of the model (top, bottom, and sides). Boundary conditions for the top or upper surface of model layers variously included MODFLOW's recharge, stream-flow routing, evapotranspiration (ET), and general-head boundary (GHB) packages. The bottom of the model was set as a no-flow boundary; we assumed that there is no appreciable exchange of groundwater between the Hooper and the underlying Midway Formations (fig. 10), both of which have a large proportion of low-permeability claystone. The updip (northwestern) boundary of each layer was also defined as a no-flow boundary. The GHB boundary package was applied to the downdip (southeast), northeast, and southwest sides of the model. The horizontal flow barrier and well packages of MODFLOW were applied internal to the model.

Table 9. Projection parameters for the model grid and hydrogeologic data.

Projection	Albers equal area conic
Units	Feet
Datum	North American Datum (NAD) 1983
Spheroid	GRS80
Central meridian	-100.00000
Reference latitude	31.25000°
First standard parallel	27.00000°
Second standard parallel	35.00000°
False easting	4921250.00000 (U.S. survey feet)
False northing	19685000.00000 (U.S. survey feet)

6.3.1 Recharge

Recharge was applied to the outcrop of each formation represented in the model, including alluvium in layer 1 and the Reklaw Formation in layer 2, as well as the parts of the Carrizo–Wilcox aquifer in layers 3 through 6. The procedure for calibrating steady-state recharge rates focused on scaling recharge rate for each outcrop cell between a minimum and maximum rate for each layer (table 10). We initially varied recharge rate also with respect to precipitation in the steady-state model. Model calibration showed, however, that higher recharge rates associated with higher precipitation rates in the north and northeast parts of the model area resulted in water levels that were simulated to be higher than measured. Recharge rate in each cell for the steady-state period (RST_{cell}) was calculated by

- (1) Estimating annual average precipitation ($P_{aver,cell}$) in each cell.
- (2) Mapping vertical hydraulic conductivity of soil (K_s ; fig. 41).
- (3) Deriving scaled soil hydraulic conductivity (K_{ss}) by linearly scaling K_s from 0 to 1, where 1 corresponds to a K_s value of 1.75 ft/d and above (every $K_s > 1.75$ ft/d is set to 1.75 ft/d). The threshold value of 1.75 ft/d was determined by examining the statistical distribution of soil conductivities.
- (4) Making initial estimates of the maximum and minimum recharge rates (R_{min} and R_{max} , respectively) for each layer. Minimum and maximum recharge rates assigned to alluvium (layer 1) cells are equal to those calculated for the underlying formation. Soil hydraulic conductivity used in the procedure for layer 1, however, is the value calculated for the soil developed on alluvium. Maximum and minimum recharge rates were adjusted during model calibration. Recharge applied to layer cells can be less than R_{min} because of the scaled soil hydraulic conductivity ($K_{ss} \leq 1$). R_{min} is the

Table 10. Calibrated values of minimum and maximum recharge rate by layer.

Unit	Layer	R_{min}^* Minimum recharge rate (inches/yr)	R_{max}^* Maximum recharge rate (inches/yr)
Reklaw	2	0.3	0.4
Calvert Bluff	3	3.33	3.91
Carrizo	4	0.8	0.8
Simsboro	5	2.6	3.9
Hooper	6	1.2	1.2

* Both R_{min} and R_{max} are maximum values; that is, for example, R_{min} is the largest minimum recharge rate that would be assigned to a cell in the layer. Few cells are assigned these upper-limit values because of scaled soil hydraulic conductivity.

maximum recharge that can be assigned to a cell that has the least precipitation in a layer. R_{max} is the maximum recharge that can be assigned to a layer's cell with the greatest precipitation.

- (5) Finding the slope and intercept (u and v , respectively) of the line that relates recharge rate $R_{s,cell}$ for each cell to average precipitation for the same cell,

$$R_{s,cell} = uP_{aver,cell} + v, \quad (5)$$

by simultaneously solving the two equations (6) and (7) that relate minimum and maximum recharge to minimum and maximum precipitation:

$$R_{min} = uP_{min} + v \quad (6)$$

and

$$R_{max} = uP_{max} + v \quad (7)$$

Minimum recharge rate corresponds to the whole outcrop minimum precipitation ($P_{min}=28.7$ inch/year), whereas maximum recharge rate corresponds to the whole outcrop maximum precipitation ($P_{max}=51.3$ inch/year). Because the steady-state model represents a long period of time (at least 100 yr), we assigned recharge using a long-term average of precipitation. Average long-term (1940 through 1997) precipitation was extrapolated for each model cell from National Weather Service station data. Station coverage was not as uniform prior to 1940.

- (6) Multiplying scaled recharge rate $R_{s,cell}$ by scaled soil hydraulic conductivity K_{SS} to obtain final cell recharge rate at steady State RST_{cell} :

$$RST_{cell} = K_{SS} \times R_{s,cell} \quad (8a)$$

$$RST_{cell} = K_{SS} \times (uP_{aver,cell} + v) \quad (8b)$$

$$RST_{cell} = K_{SS} \left(\frac{(P_{aver,cell} - P_{min})(R_{max} - R_{min})}{P_{max} - P_{min}} + R_{min} \right) \quad (9)$$

Some K_{SS} values are as low as 10^{-3} or 10^{-4} ; these cells are given small recharge rates.

For the transient model, recharge rate calculated for each outcrop cell (RTR_{cell}') differed according to each year's precipitation. Annual and monthly recharge rates were determined from scaled soil hydraulic conductivity and the difference between the actual and average precipitation rate. Transient model calibration involved adjusting the dimensionless scaling coefficient (q) relating change in scaled recharge rate $R_{s,cell}'$ and change in precipitation rate:

$$R_{s,cell}' = uP_{aver,cell} + v + q(P_{cell} - P_{aver,cell}) \quad (10a)$$

$$RTR_{cell}' = K_{SS} \times R_{s,cell}' \quad (10b)$$

$$RTR_{cell}' = K_{SS} (uP_{aver,cell} + v + q(P_{cell} - P_{aver,cell})) \quad (10c)$$

Years with higher precipitation rates were assumed to have higher recharge rates. To ensure that assigned recharge rate was positive, we set a lower limit of 0.1 inch/yr (2.3×10^{-5} ft/day) to the scaled recharge rate $R_{s,cell}'$. The actual value assigned to the model cell (RTR_{cell}) was the greater of either the calculated recharge rate or the minimum recharge of 0.1 inch/yr \times the scaled soil conductivity,

$$RTR_{cell} = \max(RTR_{cell}', 2.3 \times 10^{-5} K_{SS}) \quad (11)$$

where RTR_{cell}' , $R_{s,cell}'$, and K_{SS} are expressed in ft/day. The scaling coefficient (q) was determined by calibration procedure to be 0.06. The higher q is, the higher the range of recharge for a given cell.

For the predictive model we assigned a constant recharge rate for normal years using an average precipitation calculated from 1960 through 1997 data, excluding the effect of the

1950s drought of record from the calculation of the normal year recharge rate. Recharge rate was assigned to future drought years using equations 10 and 11 according to the difference between precipitation in those drought years and the average (1960 through 1997) precipitation rate. Monthly recharge during the drought years was kept uniform. We assumed that drainage from the unsaturated zone to the water table does not cease during a drought year.

6.3.2 Interaction of Surface Water and Groundwater

6.3.2.1 Stream-Flow Routing

All layers in this model include some number of cells in which streams or reservoirs are simulated. Both the stream-flow routing package and the reservoir package in MODFLOW use similar algorithms to simulate interaction between groundwater and surface water. For a given model cell, a water-surface elevation is assigned to the stream or reservoir, and this water level is compared with the calculated head in the aquifer. If the water level in the stream or reservoir is greater than the head in the aquifer, water will flow from the surface-water body into the aquifer as a function of the conductance of the bed sediments and the difference in heads. If the head in the aquifer is greater than the water level of the surface-water body, water will flow from the aquifer to the stream.

MODFLOW's stream-flow routing package was used to represent the interaction of groundwater and surface water in streams and river channels. The stream-flow routing package keeps track of the volume of surface water assumed to be in the river channel moving from cell to cell from upstream to downstream. Discharge from the aquifer adds to the volume of flow tracked in the river course. Water that moves from the river to the

aquifer is subtracted from the surface-water flow. The stream-flow routing package precludes water loss from exceeding the amount of water in the stream reach.

Three parameters describe the movement of water in and out of model cells: river stage, river-bottom elevation, and riverbed hydraulic conductance. We used data on surface-water stage heights from USGS gaging stations to define stream stage in the model, rather than selecting the option in the stream-flow routing package of calculating stream stage in reaches from Manning's equation. Hydraulic conductance is a function of the length, width, thickness, and hydraulic conductivity of the alluvium that transmits water between the channel and the aquifer (Harbaugh and McDonald, 1996). Length of individual stream reaches in each grid cell was measured on 1:24,000 scale USGS Topographic Quadrangle maps using an ArcView® utility. Width was estimated using several methods. For major rivers, published USGS data on river width at gaging stations (Slade, 2002) was referenced; an average of the widths from the nearest upstream and downstream gages was used throughout the outcrop reach. For smaller streams in which the width varied significantly throughout the reach, widths were increased from a few feet in the headwaters to a few tens of feet at the downstream end. Hydraulic conductivity and streambed thickness were initially estimated at one ft/d and 1 ft, respectively. Streambed conductance, assumed to be uniform along the length of any stream within each layer, was adjusted during model calibration to improve the match between simulated and targeted estimates of base flow. Streambed conductance was set over the Simsboro and Carrizo aquifers (layers 5 and 3, respectively) to values greater than those set over the Hooper, Calvert Bluff, and Reklaw aquitards (layers 6, 4, and 2, respectively). Adjustments were made for those cells that initially simulated losing reaches because, overall, the rivers are gaining across the width of

the outcrop of the Carrizo–Wilcox aquifer. Initial values of conductance also incorporated representative values of alluvium thickness. Stream flow is most sensitive to streambed conductance in a losing cell but not very sensitive to even an order-of-magnitude change in conductance in gaining cells.

Three sets of calibration targets were developed for evaluating how well the model represents interaction of surface water and groundwater. One set uses gaged information from Cibolo Creek, East Yegua Creek, Guadalupe River, Little Brazos River, Middle Yegua Creek, Navasota River, San Antonio River, San Marcos River, Tehuacana Creek, and Upper Keechi Creek. A second set uses results of low-flow studies on Cibolo Creek and the Colorado River. The third calibration set, based on the unit base-flow rate unitized per watershed in the outcrop of the Carrizo–Wilcox aquifer, is applied to the Brazos and Trinity Rivers for which gaged data for the study area were unavailable. Base flow is contributed mainly from the Simsboro and Carrizo aquifers. The unitized rates were adjusted to represent the watershed area crossing the outcrop of these aquifers.

6.3.2.2 Surface-Water Reservoirs

Any grid cell with more than half the cell area covered by surface water was represented in MODFLOW's reservoir package (figs. 54 through 59). Reservoir representation assumes that the entire grid cell is subject to inundation (that is, no partial inundation is simulated), so the length and width of reservoir cells default to the full dimensions of the grid cell. Average land-surface elevations were taken from topographic maps, whereas average water surface in the reservoirs was obtained from USGS hydrologic records. The same value of reservoir conductance was assigned to all reservoirs; there were insufficient data to do otherwise. As previously mentioned, an indirect estimate of reservoir

leakage at Lake Limestone provided a basis for assuming a reservoir conductance of 0.00001 ft/day.

6.3.3 Evapotranspiration

MODFLOW's evapotranspiration (ET) package was used, along with the stream-flow routing package, to simulate natural discharge of groundwater from the unconfined parts of the Carrizo–Wilcox aquifer (layers 6 to 3), the Reklaw aquitard (layer 2), and alluvium in layer 1. The parameters of the ET package in MODFLOW are the maximum ET rate, the elevation at which the maximum rate is applied (the ET surface), and the depth below the top of a cell at which the ET is assumed to be zero (extinction depth). Whereas the ET package is turned on for each cell representing the outcrop of a layer, groundwater discharge is indicated only if the elevation of the simulated water level is higher than the elevation of the extinction depth.

Initial values of the maximum ET rate were set to the average net lake evaporation rate (fig. 9) and varied across the outcrop. During calibration we adjusted a cutoff value to set a minimum value of 14 inches/yr for the maximum ET rate. The cutoff value applied mainly to the northeast section of the model in the Sabine Uplift area. Extinction depth was adjusted during calibration. The optimal value of extinction depth varies with cell thickness and depth to water in the cell. In the conceptual model, ET removal of groundwater occurs mainly in the river bottomlands and not across the upland surface-water divides. The net evaporation rate (pan evaporation rate minus annual precipitation) was used instead of a pan evaporation rate because the former better represents groundwater withdrawal by evapotranspiration once short-term infiltration in the unsaturated zone has been removed.

6.3.4 General-Head Boundary

The general-head boundary (GHB) package of MODFLOW is used to account for movement of water into and out of model cells. Two parameters are specified in the GHB package: GHB hydraulic conductance and hydraulic head (GHB head) at the boundary. The GHB hydraulic conductance is the proportionality constant between the flow and the difference in simulated and boundary hydraulic heads. By analogy to Darcy's Law, the proportionality constant for the northeast and southwest boundaries may be envisioned as the product of hydraulic conductivity, cell thickness, and row width, divided by column width. Thus, initial values of GHB conductance for the northeast and southwest boundaries were set equal to transmissivity. Calibration was made in the transient model to determine what value of GHB conductance gives a good calibration between simulated and observed water levels near the northeast and southwest boundaries. In transient model calibration, we determined the distance from the model edge at which simulated water levels did not respond as we adjusted GHB conductance from 0 to very large. As discussed later, the transient model responds more than the steady-state model to GHB conductance on the northeast and southwest boundaries because GHB heads there account for the effect of drawdown from groundwater withdrawal outside of the model. We interpolated transient GHB heads from maps of observed water levels in the Carrizo-Wilcox aquifer layers along the northeast model boundary. GHB conductance and transmissivity have units of length-squared/time (L^2/t).

GHB boundary cells were assigned to that part of layer 2 representing the nonoutcrop part of the Reklaw Formation to represent the exchange of groundwater between the Carrizo-Wilcox and Queen City aquifers. GHB head values represent the water level in the overlying Queen City aquifer. Values of the GHB conductance applied to layer 2 represent

the vertical hydraulic conductivity of the Reklaw aquitard. Initial GHB conductance values for layer 2 were a uniform 10^{-4} ft²/d. Water levels in the Queen City aquifer (fig. 30) have remained fairly constant during the past 50 yr, as previously discussed. Water levels are higher than in the Carrizo–Wilcox aquifer across the upland areas and lower than in the Carrizo–Wilcox aquifer in the river valleys.

The GHB package was also assigned along the downdip northeast and southwest boundaries of model layers 6 through 3, representing the Hooper aquitard, the Simsboro aquifer, the Calvert Bluff aquitard, and the Carrizo aquifer (figs. 54 through 57, respectively). The downdip boundary represents the exchange of groundwater across the Wilcox Growth Fault Zone between normally pressured and geopressed zones. For the steady-state model, we set the GHB head along the downdip boundary to match the mapped values of head shown in figures 28 and 29. The same GHB head was applied to each of these four layers. GHB conductance was assigned by trial and error. Very low values of GHB conductance, for example, less than 0.001 ft²/d, make the boundary behave as a no-flow boundary. Values of approximately 0.01 to 0.5 ft/d vary linearly along the downdip boundary from southwest to northeast. This range allows enough inflow of water from the boundary for the model to roughly match the updip-directed gradient in hydraulic head mapped across the deep Wilcox Group (figs. 28, 29). It is likely that fluid levels along the boundary have decreased locally in compartmentalized reservoirs during the past few decades owing to the withdrawal of natural gas from gas reservoirs.

The GHB boundary along the southwest side of the model was kept unchanged for the calibration and verification period representing pre-2000 conditions. This lack of change is justified by the small changes in water levels recorded in that part of the model area. The GHB boundary imposes a downdip gradient in water level in the aquifer. We varied the

GHB head assigned to the northeastern boundary of the model, accounting for the presence of well fields with large amounts of pumping just to the northeast of the study area, for example, at Tyler in Smith County. We projected predevelopment, 1980, 1990, and 2000 water-level maps for the Simsboro and Carrizo aquifers onto the northeastern boundary. We used linear interpolation to assign GHB heads for every model stress period. The GHB head for layer 4 was set to the average of the GHB heads in layers 3 and 5. Parameters for the GHB package in the transition between the hydropressured boundaries on the southwest and northeast sides of the model and the geopressured boundary on the downdip side of the model were assigned by linear interpolation.

6.3.5 Horizontal-Flow Barrier

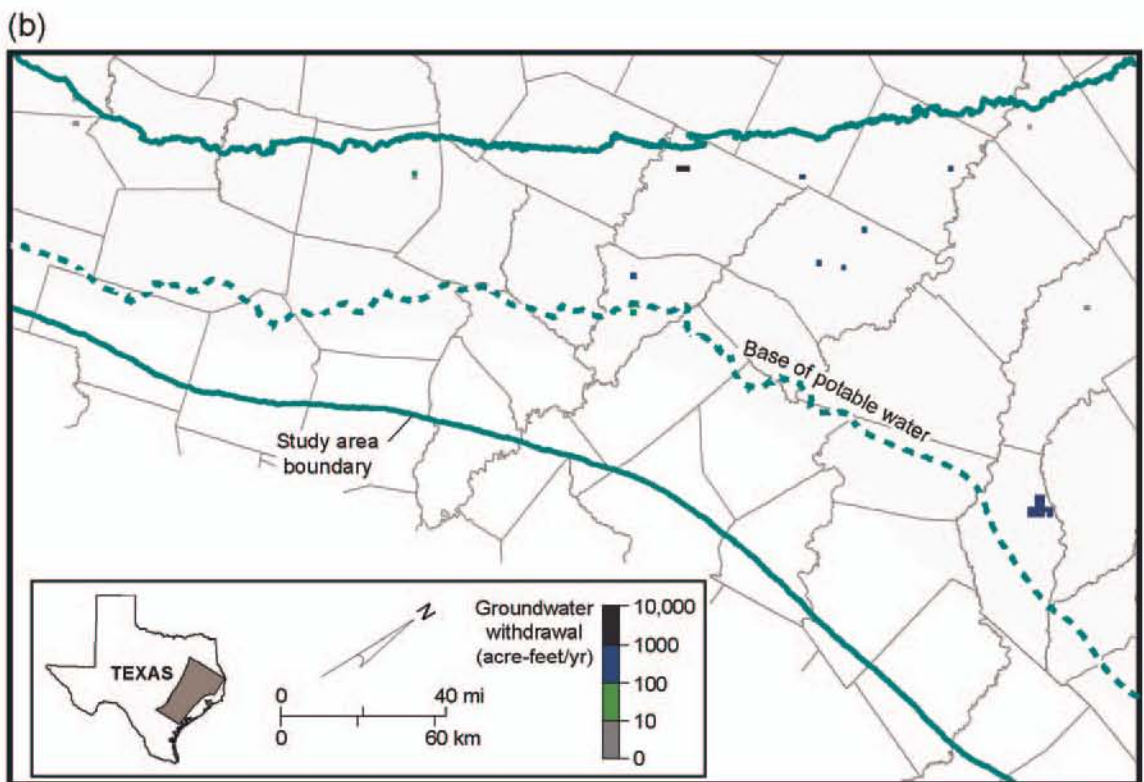
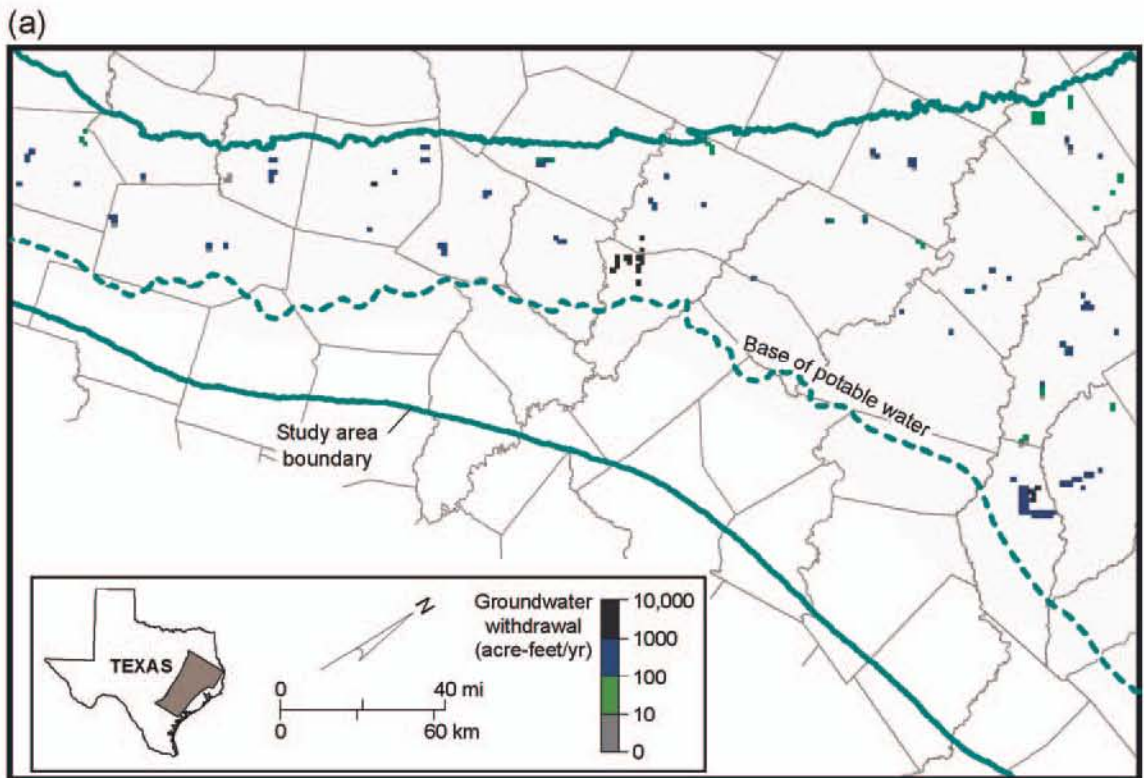
The Karnes-Milano-Mexia Fault Zone breaks up the continuity of aquifer layers between the outcrop and subsurface. Rather than attempt to vary the hydrologic properties of the individual layers of the model, we used the horizontal-flow barrier (HFB) package of MODFLOW to impede lateral movement of groundwater. Between adjacent model cells (Hsieh and Freckleton, 1993), the HFB package specifies a hydraulic characteristic term that is equal to either hydraulic conductivity divided by thickness of the barrier material (units of $1/t$) for an unconfined (variable transmissivity) zone or transmissivity divided by the thickness of the barrier material (units of L/t) for a confined (constant transmissivity) zone. The HFB boundary was applied both to the updip normal faults with down-to-the-coast displacement, where blocks of Calvert Bluff, for example, are juxtaposed adjacent to high-permeability Simsboro material, and to the antithetic faults that form the southeastern side of the grabens typical of this extensional fault zone. The HFB package was applied to all layers (figs. 54 through 58) except for layer 1, representing alluvium. Dutton (1999) also used the

HFB package and varied HFB hydraulic characteristic proportional to the amount of throw on the several major fault strands included in his model. This model of the central part of the Carrizo–Wilcox aquifer includes a greater number of HFB cells; uniform conductances were applied regardless of fault displacement. The hydraulic characteristic of the fault zone was adjusted during model calibration. Initial estimates of the HFB hydraulic characteristic were 2×10^{-4} ft/d for cells in the confined part of the Carrizo–Wilcox aquifer, and 2×10^{-5} d⁻¹ for cells in the unconfined part.

6.3.6 Wells

Groundwater withdrawal for municipal, manufacturing, and power uses was associated with specific wells identified by the water user group. In some cases we had to assume a location of a well, especially for the predictive model. Total annual pumping by user group was prorated equally among all identified wells for that group. Figure 60a, b shows the allocation of pumping assigned to the model to represent municipal and manufacturing water supplies in 2000.

Pumping for irrigation, mining, rural domestic, and stock uses was distributed areally on the basis of land use and other information (fig. 60c–f). Irrigation was distributed mainly on the basis of Geographic Information Systems (GIS) coverages from 1989 and 1994 TWDB surveys. Some irrigated tracts of land are identified in both surveys; some land is designated as irrigated on only one survey. We made the assumption that any parcel of land identified in either survey constituted an area where groundwater was extracted for irrigation. We excluded areas where identified irrigation land falls within boundaries of municipal (population more than 500) areas. Some counties have listed irrigation use but no land



QAd2287(a)x

Figure 60. Distribution of groundwater withdrawal in 2000 for (a) municipal and (b) manufacturing and power supplies.

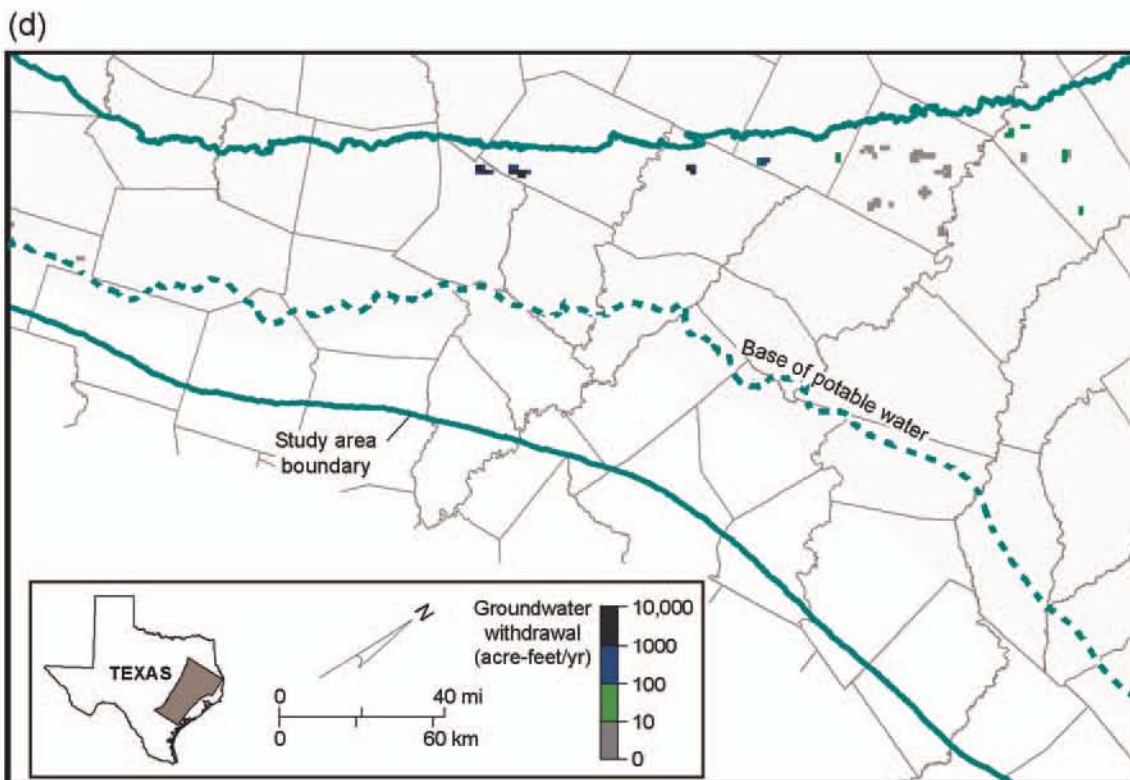
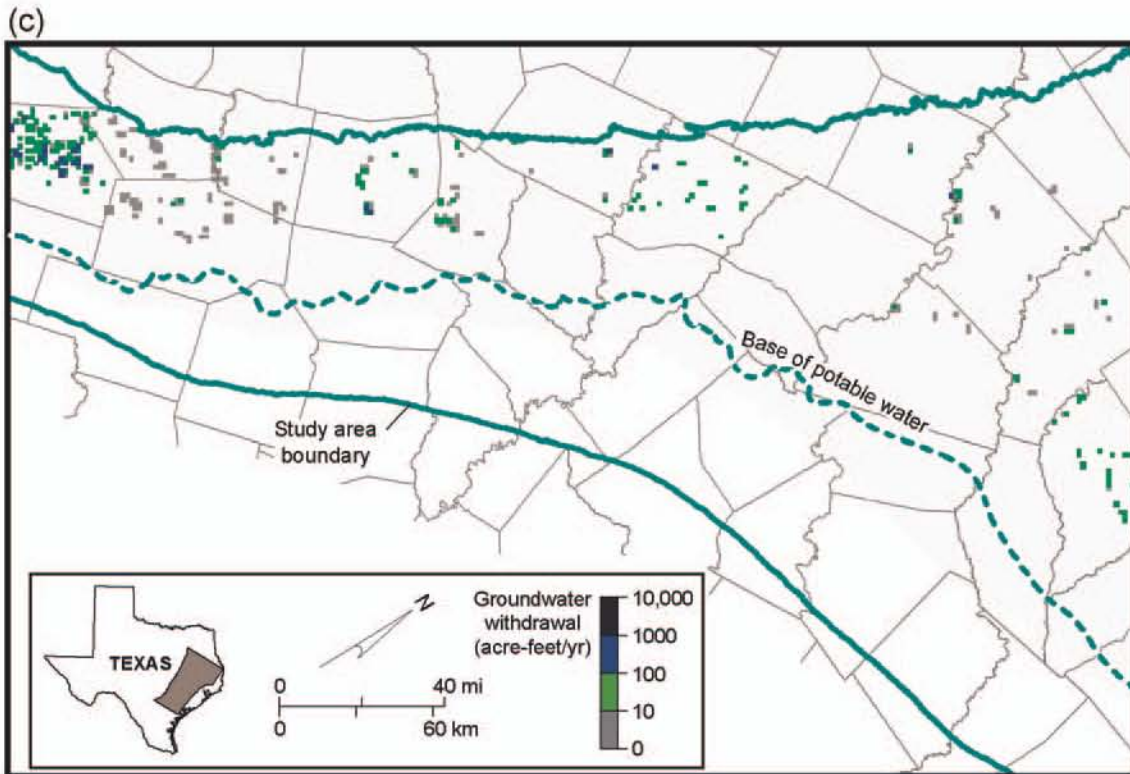
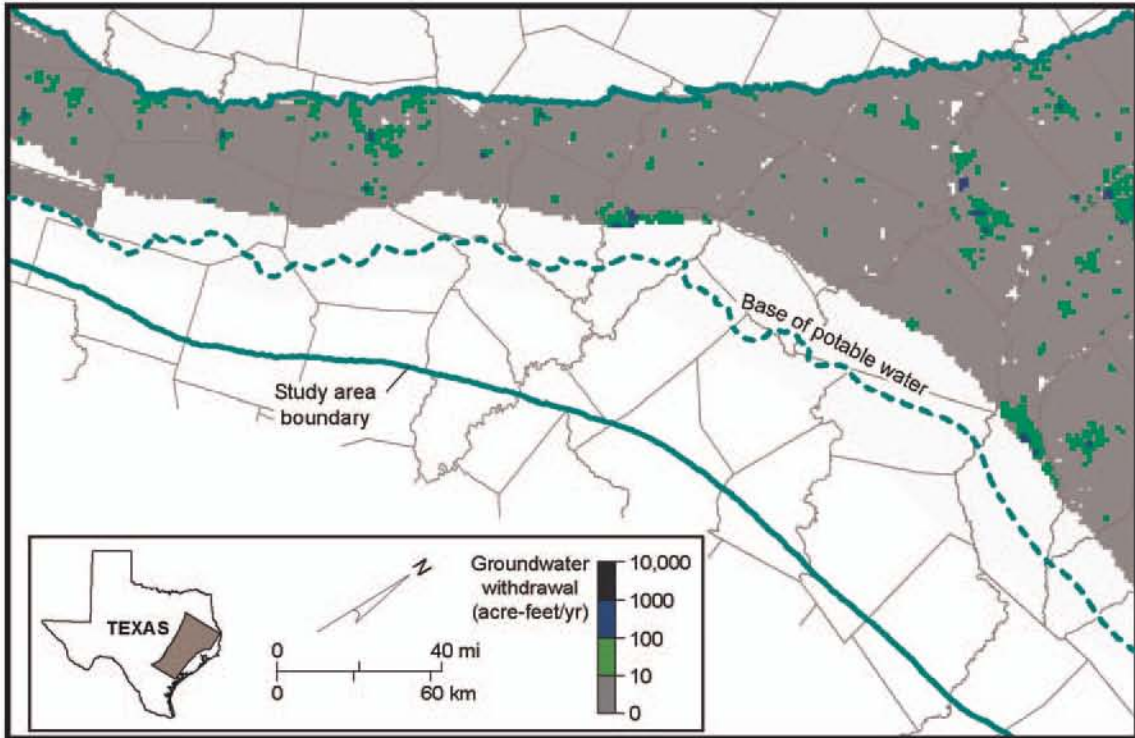
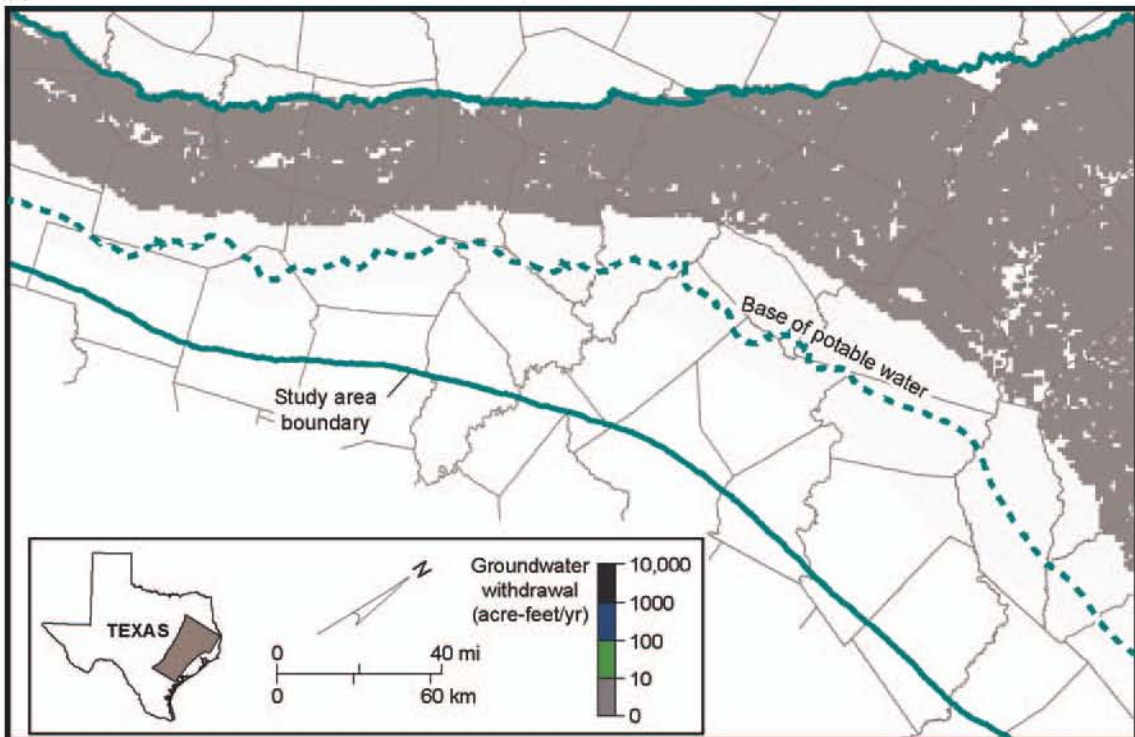


Figure 60 (continued). Distribution of groundwater withdrawal in 2000 for (c) irrigation supply and (d) mining-associated activity.

(e)



(f)



QAd2287(c)x

Figure 60 (continued). Distribution of groundwater withdrawal in 2000 for (e) rural domestic and (f) livestock supplies.

identified in the 1989 or 1994 survey. For these counties we distributed pumping to irrigation water wells included in the TWDB online groundwater database.

Groundwater extraction for mining (fig. 60d) was assigned using partly land-use information presented in GIS format and partly additional information. Land use for which groundwater was assumed to have been produced for mining included strip mines, quarries, and gravel pits. Information on groundwater extraction rates at the Sandow Mine in Milam County, the Three Oaks Mine in Lee County, and the Walnut Creek Mine in Robertson County was based on information contained in permit files at the Railroad Commission of Texas (Bob Harden, 2001, written communication).

Rural domestic use was distributed on the basis of 1990 and 2000 census results (fig. 61). Population in census tracts, excluding municipal areas with more than 500 people, was linked to the grid of model cells. Population was linearly interpolated for model cells between 1990 and 2000. Population before 1990 was prorated by the ratio of county-total population in the year of interest to the 1990 population. Rural domestic water use was distributed to model cells (fig. 60e) on the basis of the proportion of total population accounted for by each model-cell area.

Stock water use (fig. 60f) was mapped according to land-use information also presented in GIS format. Groundwater extraction for stock watering was assigned for parcels identified as having land uses of (1) cropland and pasture, (2) confined feeding operations, or (3) herbaceous, shrub and brush, and mixed rangeland. Acreage associated with each mapped land parcel was totaled per county. County total groundwater use was prorated to individual parcels on the basis of their percentage of county totals. The land-use coverage was for the mid-1970s to early 1980s. We assumed that these water uses had the same proportional distribution in other years included in the model.

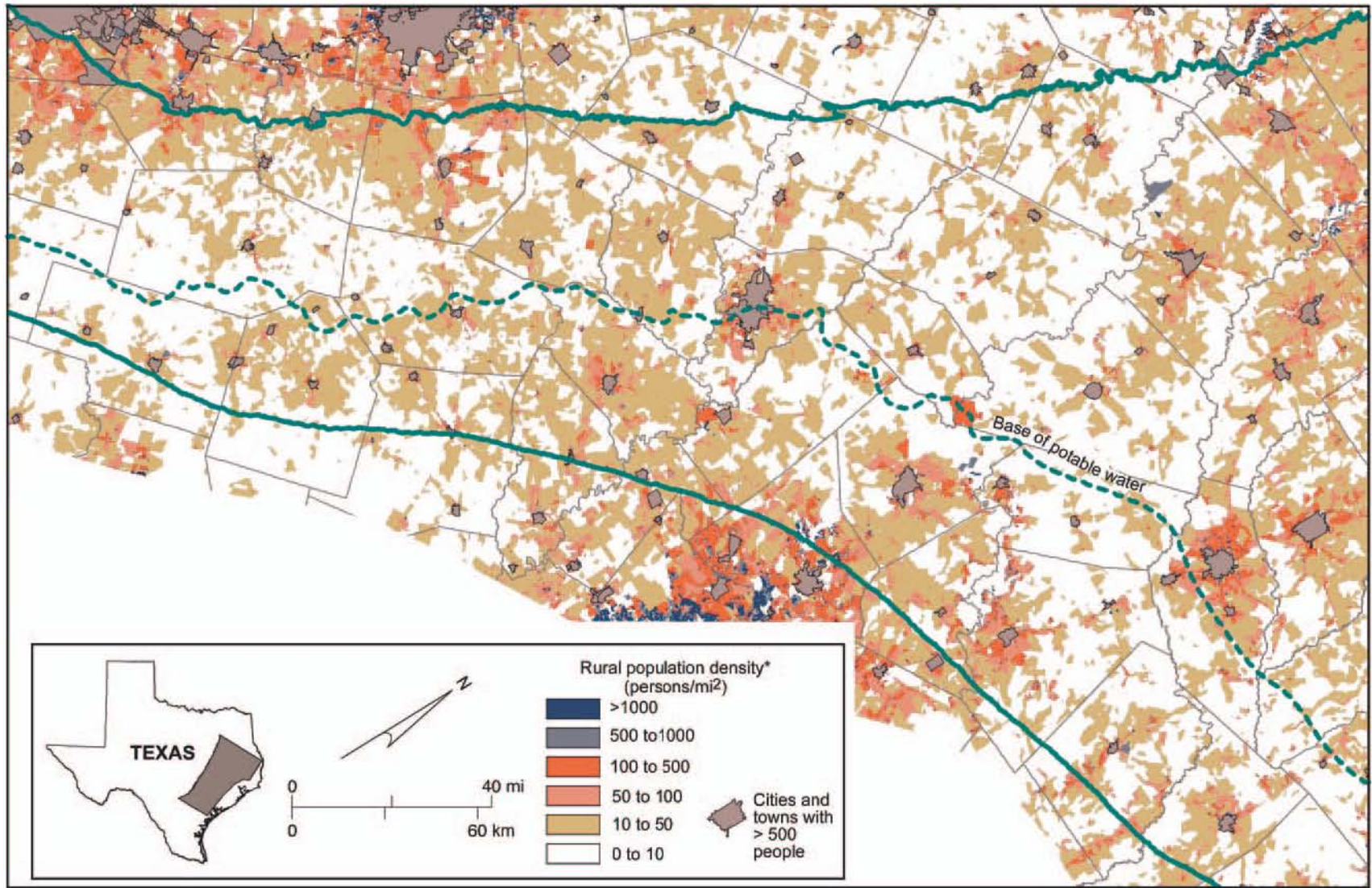


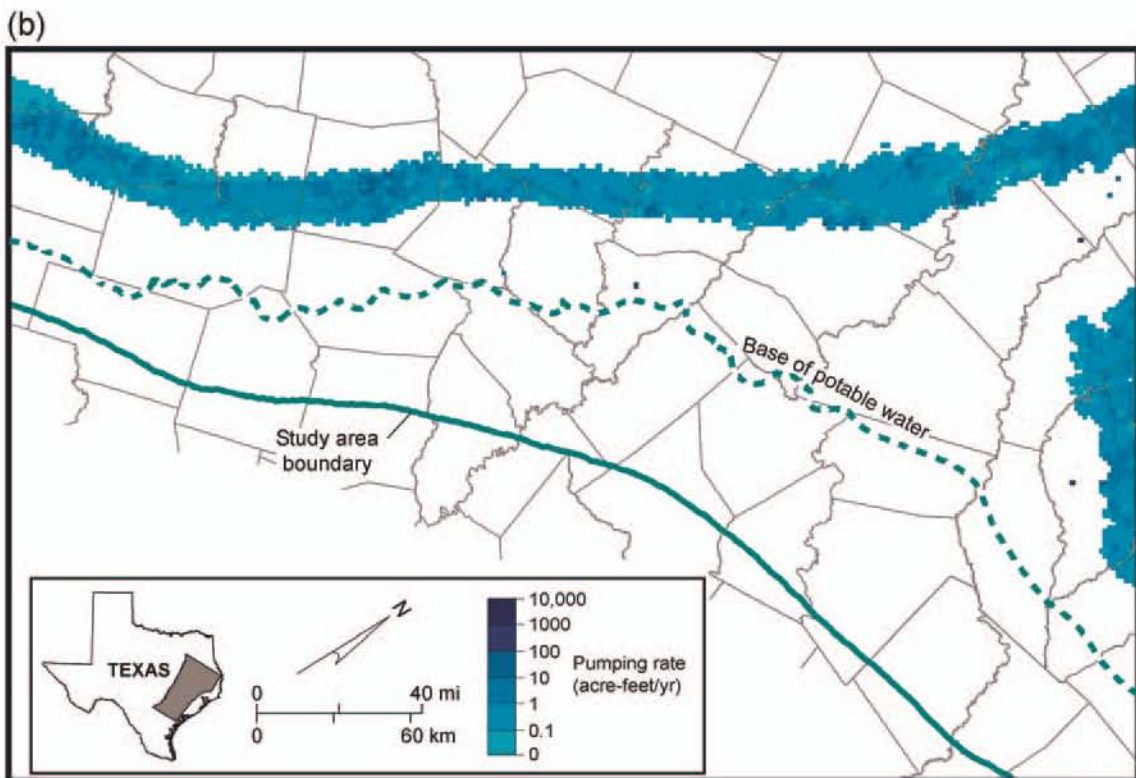
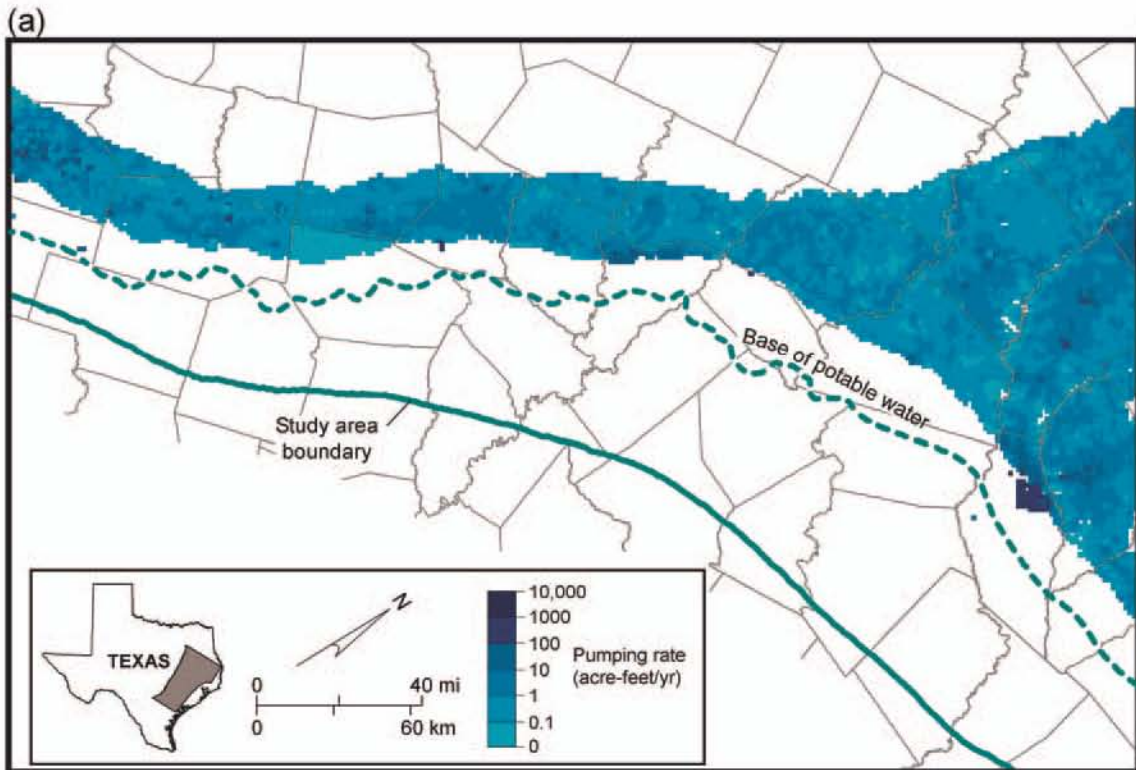
Figure 61. Map of population density in rural parts of the study area, excluding cities and towns with more than 500 people.

QAd1811(f)c

Pumping allocated by well was assigned to model layers on the basis of well information where available. Well information in the TWDB groundwater database can include aquifer, well depth, and screen interval. We cross checked the elevation of the well bottom against elevations of the top and bottom of model cells where wells were assigned. In some cases results did not agree with the aquifer designation. For some wells we assigned model layer on the basis of assignments for other nearby wells.

Pumping used for rural domestic, stock, and irrigation was assigned to model layer (figs. 62, 63) on the basis of well depth. We assumed that few wells for rural domestic, stock, or irrigation would be completed in the Hooper or the Calvert Bluff aquitards if the wells could be completed in the Simsboro or Carrizo aquifer, respectively. Also, we assumed that where depth to the Carrizo aquifer increased, rural domestic, stock, and irrigation wells would be drilled into the overlying Queen City aquifer. This assumption resulted in a downdip limit of pumping in each model layer for rural domestic, stock, and irrigation uses. Pumping was also split between the Carrizo and Simsboro aquifers in part of the East Texas Basin and in Bastrop County (figs. 62, 63).

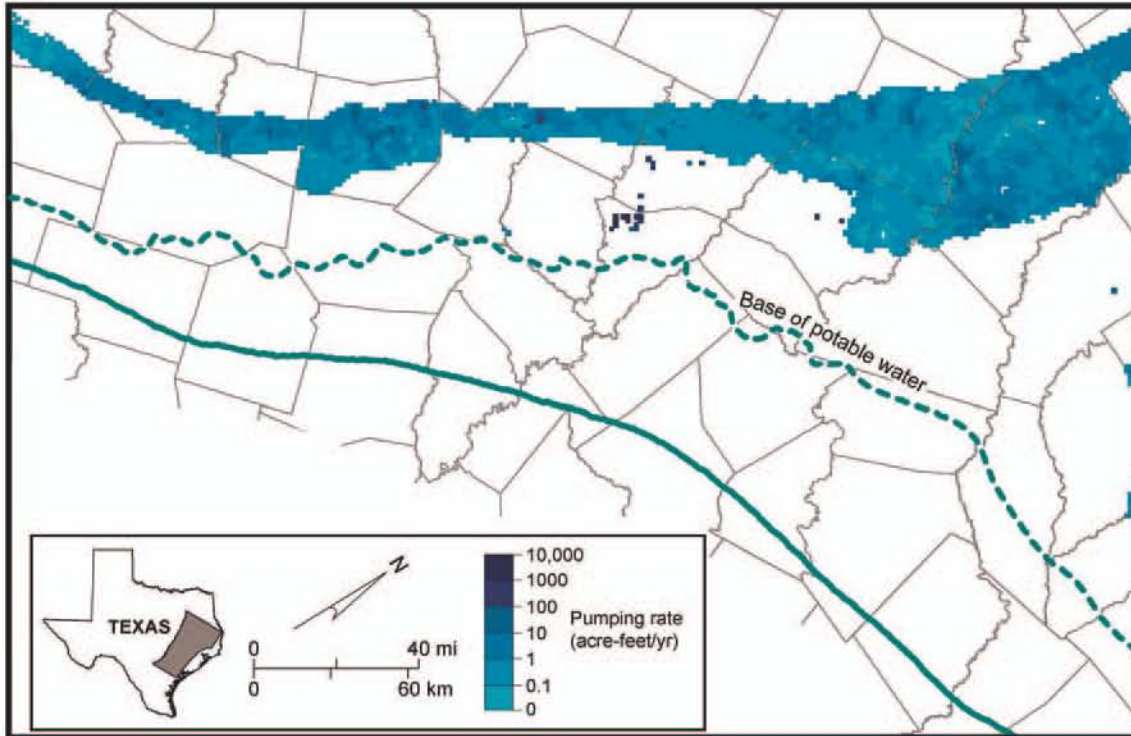
Pumping in the Lufkin-Angelina County well field occurs at the downdip limit of pumping in layer 3, approximately 10 mi from the limit of potable water in the Carrizo–Wilcox aquifer (figs. 62a, 63a). Depth to the top of the Carrizo aquifer in the well field is more than 900 ft. No pumping was assigned to the deepest, downdip part of the aquifer, as previously explained. Likewise, pumping from the downdip part of the Calvert Bluff aquitard is assumed to be limited where the aquifer is overlain by the full section of the Carrizo aquifer (figs. 62b, 63b). The Bryan-College Station well field straddles the line between Brazos and Robertson Counties. We assumed that most pumping from the Hooper aquitard is generally near its outcrop because of the depth of drilling and water quality. Individual wells



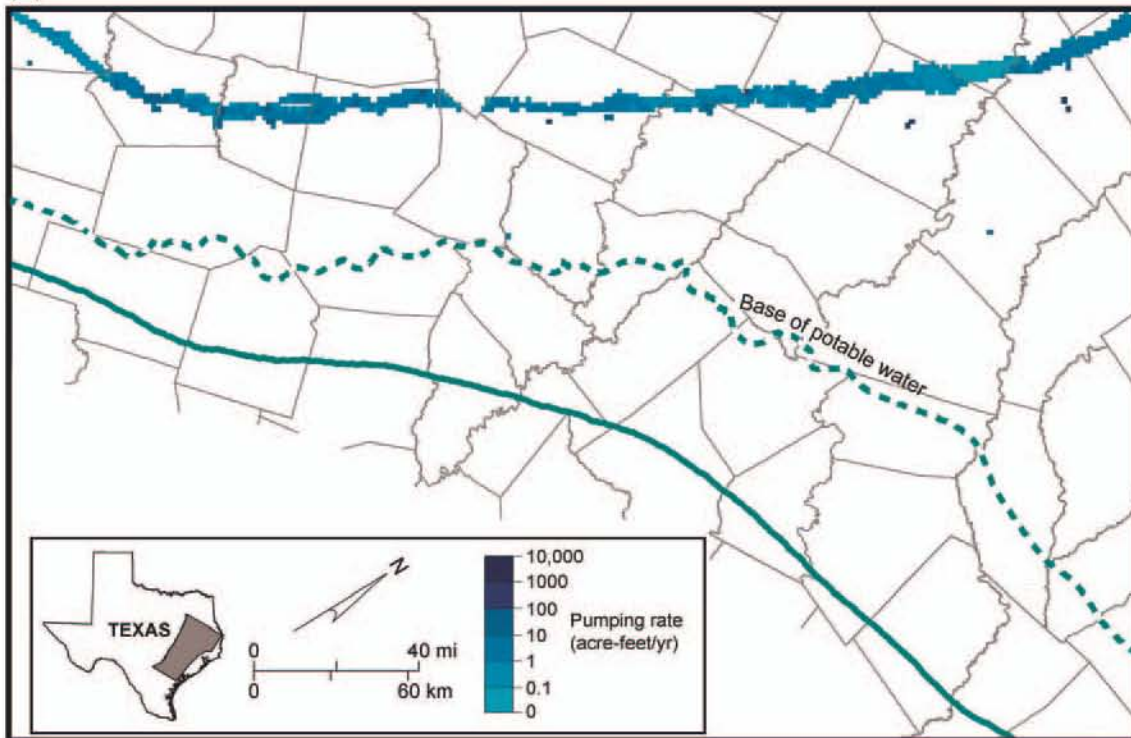
QAAd2053(a)/c

Figure 62. Variation in total rate of groundwater withdrawal in 1990 in (a) Carrizo aquifer and (b) Calvert Bluff aquitard.

(c)



(d)



QAd2053(b)jc

Figure 62 (continued). Variation in total rate of groundwater withdrawal in 1990 in (c) Simsboro aquifer and (d) Hooper aquitard.

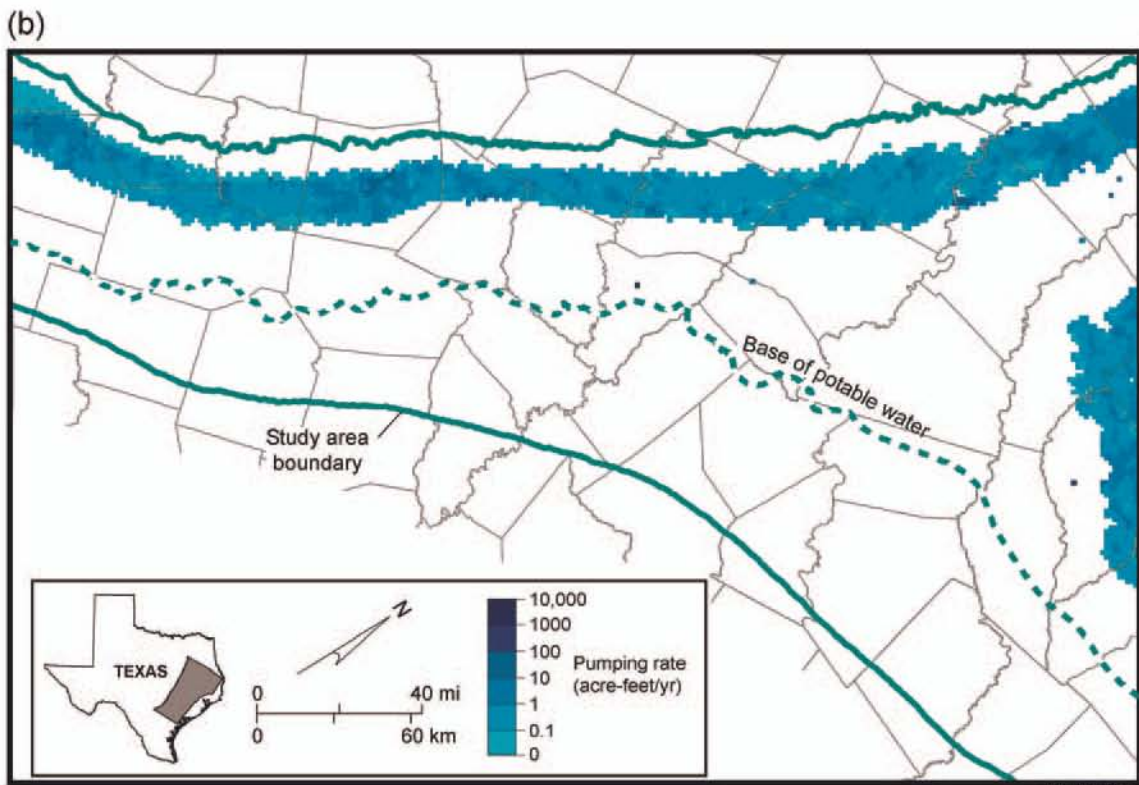
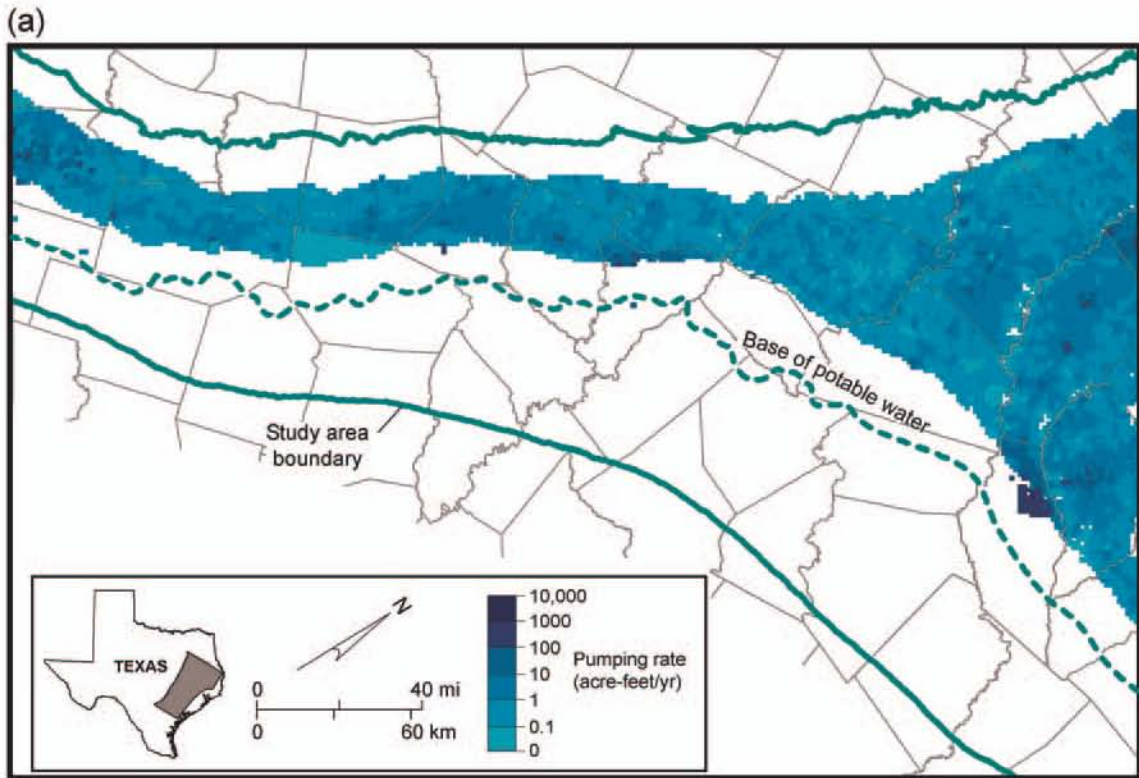


Figure 63. Variation in total rate of groundwater withdrawal in 2000 in (a) Carrizo aquifer and (b) Calvert Bluff aquitard.

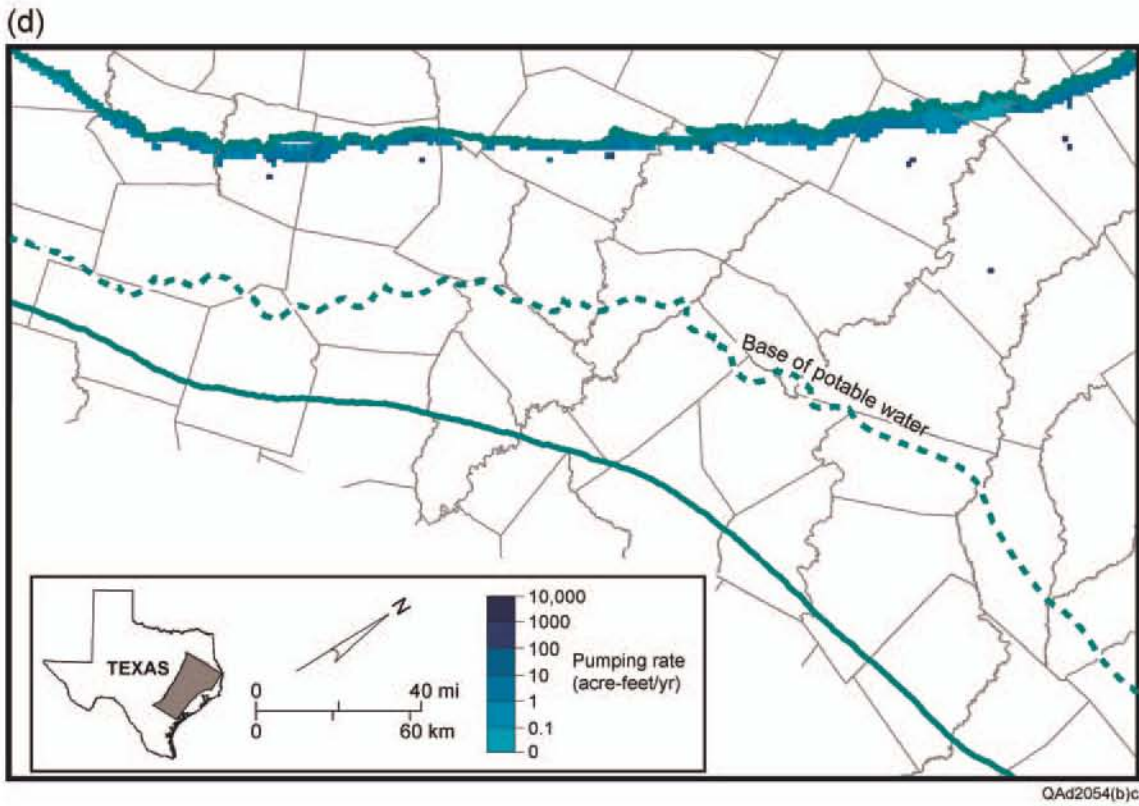
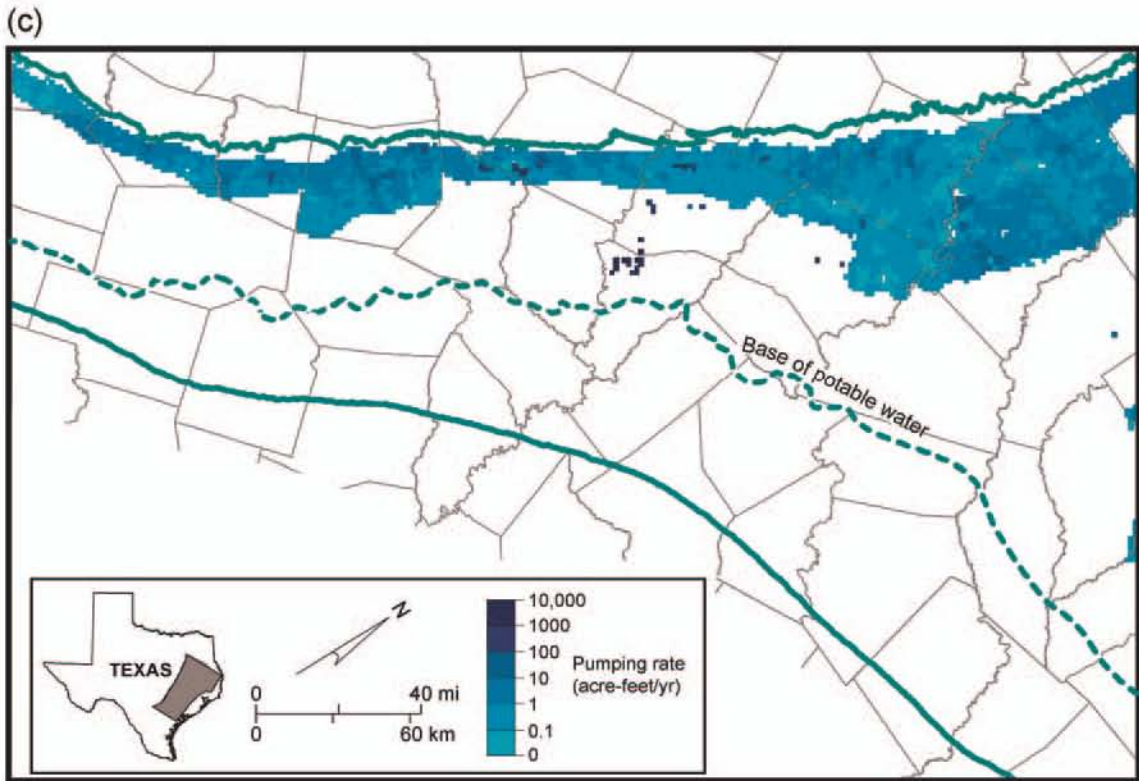


Figure 63 (continued). Variation in total rate of groundwater withdrawal in 2000 in (c) Simsboro aquifer and (d) Hooper aquitard.

in Freestone, Anderson, and Henderson Counties in the Hooper aquitard are deeper and show that this assumption is not valid everywhere.

The TWDB developed predictive pumpage data sets for 2000, 2010, 2020, 2030, 2040, and 2050, subdivided into seven water-use categories. The source of the data sets was water-demand projections from the regional water plans as contained in Volume II of the 2002 State Water Plan (SWP) (TWDB, 2002). TWDB compared demand projections, currently available supplies, and associated strategies for water user groups listed in the SWP for the 2000-through-2050 planning cycle. TWDB adjusted predicted pumpage estimates so that the value to be used in the various GAM models did not exceed projected demands. Records associated with groundwater use were assigned to various aquifers.

The various regional water plans present information on how future supplies from the Carrizo–Wilcox aquifer will be obtained, such as by drilling one or more additional wells to expand a city’s well field. Other plans do not provide specific information. Where additional wells are specifically mentioned, we added scheduled groundwater withdrawal to cells located in the vicinity of the well field. If additional wells were not targeted as a strategy, we simply increased the pumping rate from the enumerated wells in a city’s well field. Similarly, new groundwater withdrawal for manufacturing was assigned to model cells in appropriate locations. Increases in groundwater withdrawal for power was simulated by increased pumping from previously used model cells. Changes in pumping for irrigation, mining, rural domestic, and stock water uses were generally handled by prorating the amounts across the cells used in the 2000 simulation unless other information was available.

The Region K regional water plan identified the Carrizo–Wilcox aquifer as a water-management strategy for the City of Pflugerville in Travis County. The TWDB pumping rate for this strategy ranges from 700 acre-ft/yr in 2000 to 1,453 acre-ft/yr in 2050. This pumping

was assigned to the Simsboro aquifer in the vicinity of Elgin, Bastrop County, which is the productive area of the aquifer nearest the City of Pflugerville.

The Region G regional water plan identified the Carrizo–Wilcox aquifer as a water-management strategy to meet Williamson County water needs. Predicted groundwater withdrawal ranges from less than 1,000 acre-ft/yr in 2001 to more than 18,000 acre-ft/yr in 2050. Identified users included the cities of Bartlett, Brushy Creek, Florence, Georgetown, Granger, Hutto, Leander, Round Rock, Taylor, and Thrall, as well as water-supply corporations supplying rural domestic users. This predicted groundwater withdrawal was split between the Carrizo and Simsboro aquifers and allocated in the model to Lee County using the footprint defined in the Trans-Texas Water Program (HDR Engineering, 1998) and previously simulated in the Dutton (1999) model.

The Region L regional water plan identified the Carrizo–Wilcox aquifer as part of several water-management strategies to meet water needs for the City of San Antonio. In late 1998, a contract between Alcoa Inc. (ALCOA), San Antonio Water System (SAWS), and San Antonio’s City Public Service (CPS) was announced for transfer of groundwater produced from mining operations in Bastrop, Lee, and Milam Counties to provide municipal water supply to the City of San Antonio. Previously, groundwater extracted from the Simsboro aquifer as part of mining operations was discharged and released as surface water. Most of that released water would be transferred to SAWS. Additional pumping beyond that required for mining operations, however, was anticipated. This transfer was adopted as water-management strategy Simsboro SCTN-3 in the South Central Texas Region L water plan. The rate specified in the TWDB City Municipal Master Predictive data set for this strategy is approximately 50,600 acre-ft/yr in 2000, decreasing to about 31,500 acre-ft/yr in 2010, and then gradually increasing to about 38,700 acre-ft/yr in 2050.

To allocate this groundwater withdrawal, we assumed the total SAWS transfer would always be greater than the amount being pumped as part of mining operations, requiring additional pumping. We determined the additional amount of groundwater withdrawal needed to meet the targeted amount for transfer and allocated that amount to cells representing the Simsboro aquifer in the vicinity of the projected mining operations around the Sandow and Three Oaks mines in Bastrop, Lee, and Milam Counties. We assumed that 5,000 acre-ft/yr of ground water would be retained by ALCOA for on-site use.

Additional Region L water-management strategies referred to as the Carrizo aquifer–Gonzales and Bastrop (CZ-10D) plan and the Carrizo aquifer–Schertz-Seguin Water Supply Project identified the Carrizo–Wilcox aquifer in Gonzales County as a source of groundwater for municipal, manufacturing, and power-generation needs. This withdrawal was assigned to the Carrizo aquifer in the western part of Gonzales County. Model cells were designated for the simulation with the assistance of the Gonzales County Conservation District.

6.4 Model Parameters

Model parameters, including elevations of the top and bottom of layers, horizontal and vertical hydraulic conductivities, coefficient of storage (storativity), and specific yield, were distributed and assigned to model cells using a combination of Surfer® and ArcView®, and Microsoft Excel.

The top and bottom of layers were mapped from a digital database. Merging of the spatially dissimilar data sets required the use of geographic information systems (GIS) and geostatistical software packages. Once compiled, initial layer elevation data sets were checked for vertical consistency through surface subtraction using the triangulated irregular

network method of surface interpolation. Insertion of control points at appropriate locations corrected areas showing vertical discrepancies. Geostatistical methods were used to interpolate the structure surface across that part of the model with sparse or no data. This process included calculation of layer thickness, kriging the thickness surface throughout the model area, recalculation of layer boundary elevation from the kriged surface, and merging the recalculated elevation surface into data-poor zones. The complete layer boundary elevation surfaces were then draped onto points representing the model cell centroids. Particular attention was made to improving the accuracy of structural mapping across the Karnes-Milano-Mexia Fault Zone and in extrapolating the structural surfaces across the outcrop where the formations thin. Mapping of structure surfaces was coordinated for the central, southern, and northern GAM models of the Carrizo–Wilcox aquifer to ensure consistency.

We used Surfer® to interpolate gridded values of hydraulic conductivity. Input files for each layer included the measured data from Mace and others (2000c) and digitized traces of contours of hydraulic conductivity hand drawn by a geologist to take into account variations in thickness of sandstones. Once we had values of horizontal hydraulic conductivity, layer thickness, and sandstone thickness assigned to each model cell, we used a Fortran program to calculate equations 3 and 4 for horizontal and vertical hydraulic conductivity for the cells. Further adjustment was needed to match calculated values to well-known values, for example, in the vicinity of the Bryan-College Station well field. Other adjustments were made where initially calculated values appeared much higher than the statistical distribution (Mace and others, 2000c) would predict. We set the upper limit of hydraulic conductivity in the Simsboro aquifer to approximately 30 ft/d. Further corrections were needed to extrapolate results across the outcrop.

MODFLOW uses the dimensionless coefficient of storage, or storativity, to determine the volume of water released from a vertical column of a model layer per unit surface area and unit decline in hydraulic head. For cells in which the simulated hydraulic head is below the top of a cell, for example, cells representing the unconfined aquifer in the outcrop, MODFLOW switches to using specific yield to determine the volume of water released from a vertical column of a model layer per unit surface area and unit decline in hydraulic head. Storativity is a function of porosity, compressibility of water, and elasticity of the formation. We assumed that rock elasticity decreases as the sediment undergoes compaction and lithification during burial. Detrital minerals dissolve and additional minerals precipitate as cement in the pores of sediment, further changing porosity (Loucks and others, 1986) and elasticity. We accordingly varied storativity as a function of depth and texture of the aquifer matrix (for example, sandstone versus claystone).

Calibration involved specifying the range between maximum storativity at shallow depth and minimum storativity at greater depth and the effect of sand content. The calibrated model used a maximum baseline storativity of $10^{-3.5}$ (3.16×10^{-4}) at the updip edge of the confined aquifer in each layer and a minimum baseline storativity of $10^{-4.5}$ (3.16×10^{-5}) at the downdip limit of potable water (figs. 64 through 67). The more saline zone at depth was assigned a baseline storativity of $10^{-4.5}$. Storativity of the confined part of the Reklaw aquitard was also set to a uniform $10^{-4.5}$ (fig. 68). Storativity assigned in the model (S) for the Carrizo–Wilcox aquifer was adjusted from the baseline value (S_z) to reflect sand content in each layer using equation 12:

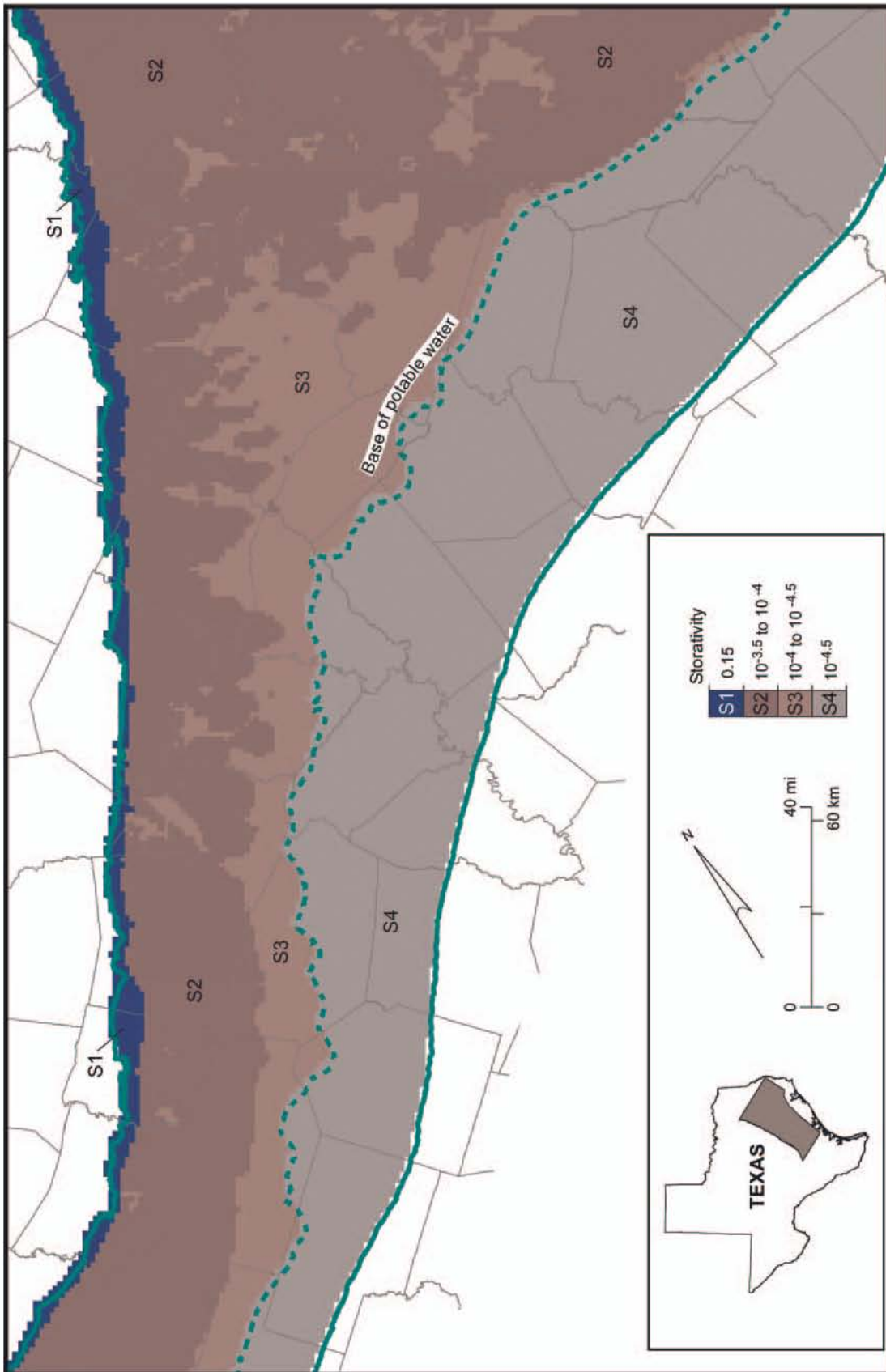
$$\begin{aligned} \text{Log}(S) &= \text{Log}(S_z) + \text{SPF}, \text{ where} \\ \text{SPF} &= (0.5 - \text{Sand content})/0.5 \end{aligned} \tag{12}$$

As *Sand content* for any cell of the model layer approaches 100 percent, the *SPF* term goes to -1 and reduces storativity by an order of magnitude. Likewise, as *Sand content* approaches 0 percent, the *SPF* term goes to 1 and increases storativity by an order of magnitude.

Specific yield was set to 0.15 for the Simsboro and Carrizo aquifers and to 0.10 for the Hooper, Calvert Bluff, and Reklaw aquitards. Specific yield of alluvium (layer 1) and of the additional cells in layers beneath the alluvium was set to 0.25.

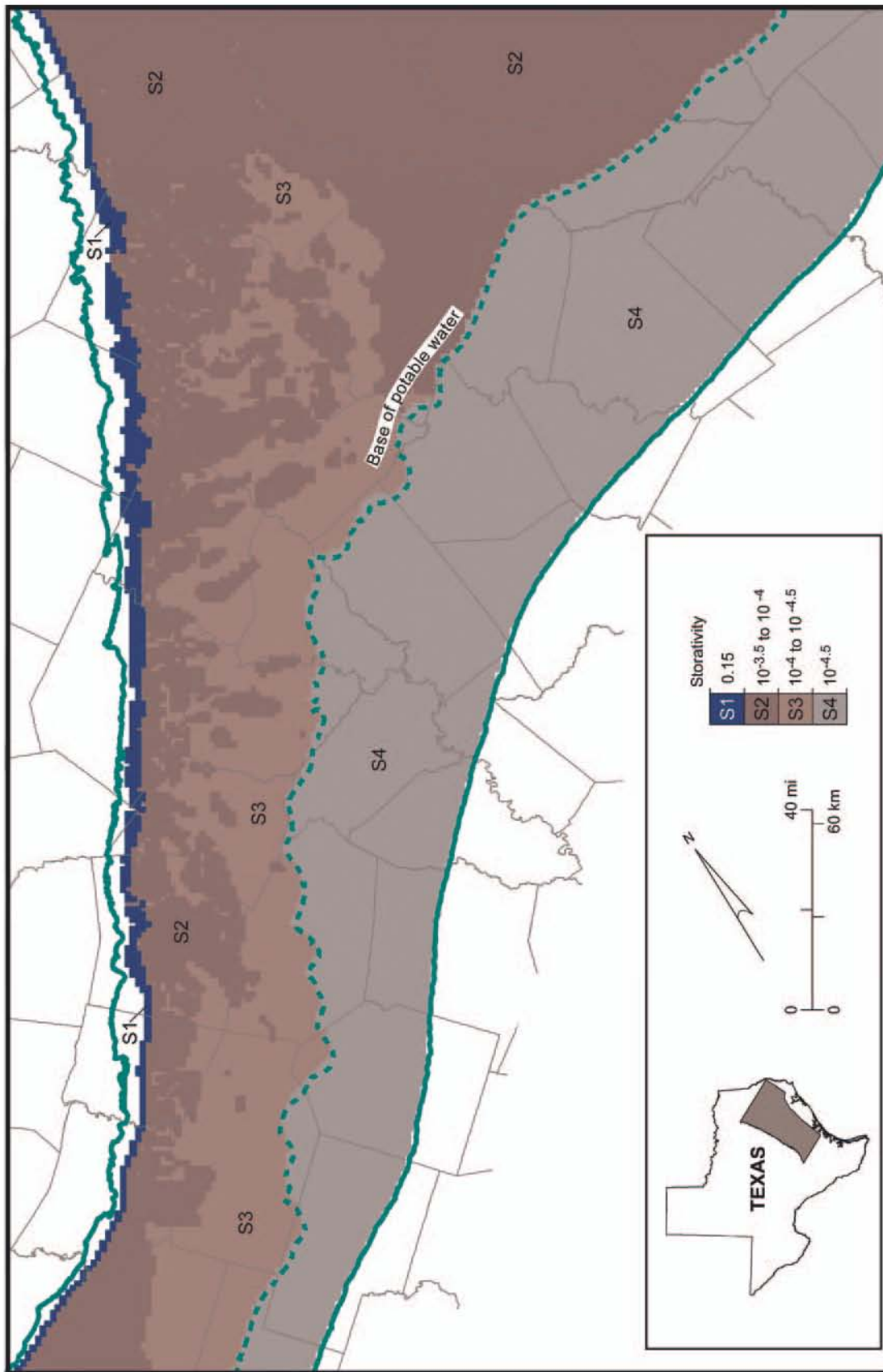
We made layer 1, representing the alluvium, an unconfined layer in which transmissivity varies with saturated thickness. The additional cells in layers 2 through 5 beneath the alluvium of layer 1 were considered extensions of the alluvium and were given a thickness of 0.1 ft. Because water level must lie above the top of these cells, that is, within the alluvium cells in layer 1, the additional cells in layers 2 through 5 are specified as confined but given a storage coefficient equal to that of the alluvium (0.25). In initial simulations, however, setting horizontal and vertical hydraulic conductivities of the additional cells equal to those of layer 1 increased the convergence time required for the simulation. Accordingly, the calibrated horizontal and vertical hydraulic conductivities of the additional cells were set to 1 ft/d.

Layers 2 through 6 were set as confined/unconfined. We allowed MODFLOW to calculate transmissivity from input values of hydraulic conductivity and layer and saturated thickness as appropriate. Storativity was specified as a model input. We used the Strongly Implicit Procedure (SIP) with a convergence criterion of 0.001 ft.



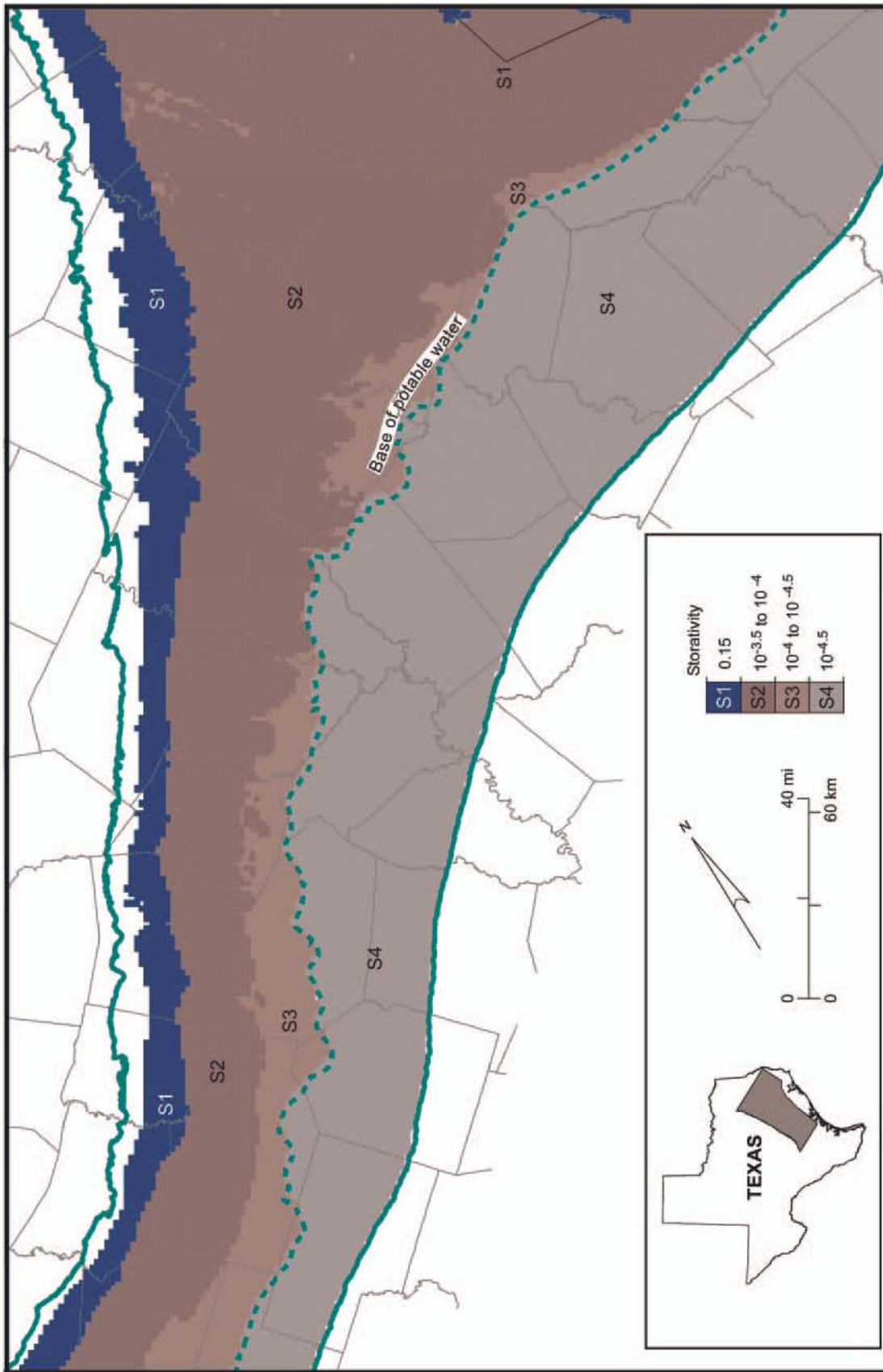
QA0278(a)c

Figure 64. Storativity assigned to model cells representing the Hooper aquard (layer 6).



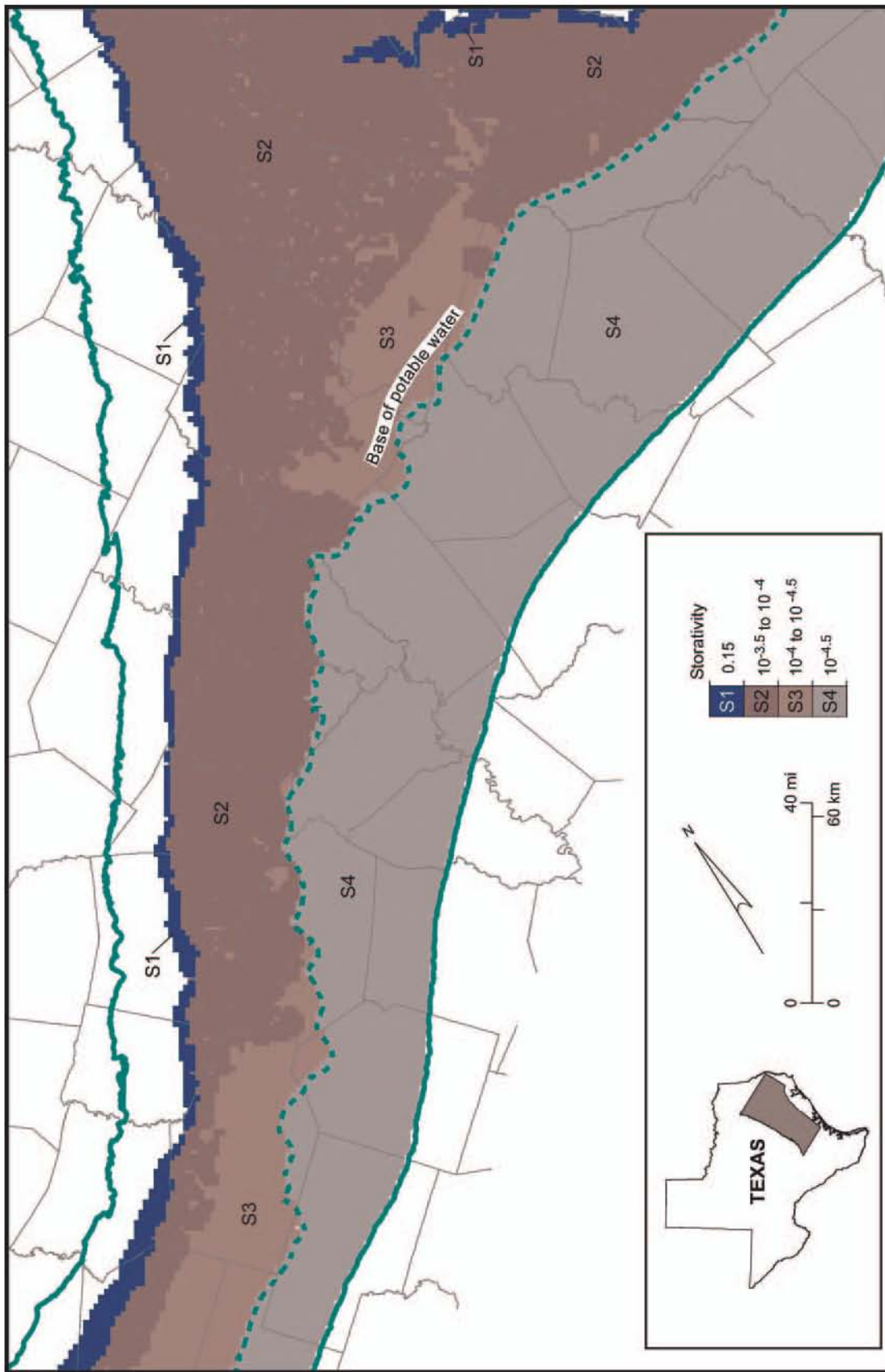
QA02278(b)c

Figure 65. Storativity assigned to model cells representing the Simsboro aquifer (layer 5).



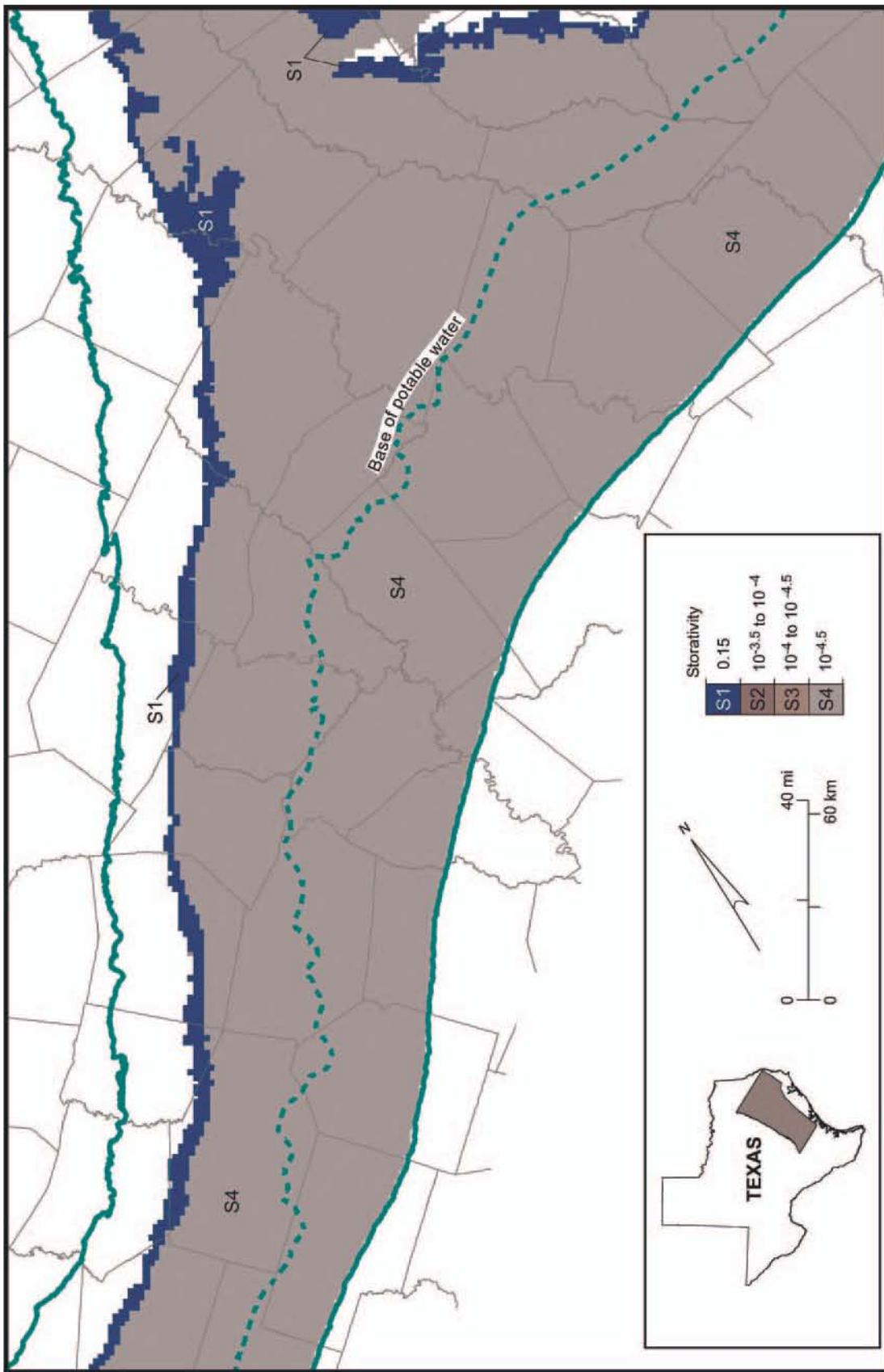
QA4278(c)

Figure 66. Storage assigned to model cells representing the Calvert Bluff aquitard (layer 4).



QAd2278(d)bc

Figure 67. Storativity assigned to model cells representing the Carrizo aquifer (layer 3).



QAd278(e)jc

Figure 68. Storativity assigned to model cells representing the Reklaw aquitard (layer 2).

7.0 MODELING APPROACH

The modeling sequence included

- (1) Setting up and calibrating the steady-state version of the model. The steady-state model was used to make initial adjustments of model parameters, including hydraulic conductivities, recharge, parameters for the stream-flow routing and ET packages, GHB boundaries, and horizontal-flow barrier (HFB) parameters.
- (2) We set up a transient version of the model for calibration against the period of record from 1950 through 1990, with emphasis on the last 10 yr. We included pumping for the early part of the period at approximately the same rate as in 1980. We assumed that pumping rates did not vary greatly during this period, except in the well fields, and variation was estimated from changes in population. Moving the starting date for the transient model to 1950 decreases the influence of initial conditions on model results for the 1990 calibration. During the calibration phase we made further adjustments to all model parameters, including storativity.
- (3) The verification period ran from 1991 through 2000. Results for this period suggest how well the model may perform as a predictive tool.
- (4) The model was used to predict water-level changes during the period from 2000 through 2050 as an example of its use in predicting future conditions in the aquifer. Pumping rates for the predictive simulations were developed by the TWDB from Regional Water Planning Group projections. We used average recharge rates for predictive stress periods except for the last 36 month-long stress periods of each simulation.

The steady-state model was first established using the steady-state solution feature of MODFLOW. The steady-state model later was combined with the transient model and solved in a 100-yr stress period (effectively 1851 through 1950) with 200 time steps. The transient model for 1951 through 1990 and 1991 through 2000 was run with 1-yr stress periods, except that month-long stress periods were included for the drought years of the 1980s (1987 through 1989) and the 1990s (1995 through 1997). Most stress periods were solved using one time step with fewer than 200 iterations. For some stress periods in which pumping rates changed appreciably we had to increase the number of time steps to ensure convergence; at most, 5 time steps were used for annual stress periods or 10 time steps for month-long stress periods.

The 2000-through-2050 predictive simulations included a number of runs:

- (1) a run for 2000 through 2010, with 120 month-long stress periods, ending with drought-of-record recharge rates for the last 36 month-long periods (2007 through 2010);
- (2) a run for 2000 through 2020, with 10 annual stress periods, followed by 120 month-long stress periods, and ending with drought-of-record recharge rates for the last 36 month-long periods (2018 to 2020);
- (3) a run for 2000 through 2030, with 20 annual stress periods, followed by 120 month-long stress periods, and ending with drought-of-record recharge rates for the last 36 month-long periods (2028 through 2030);
- (4) a run for 2000 through 2040, with 30 annual stress periods followed by 120 month-long stress periods, and ending with drought-of-record recharge rates for the last 36 month-long periods (2038 through 2040);

- (5) a run for 2000 through 2050, with 40 annual stress periods, followed by 120 month-long stress periods, and ending with drought-of-record recharge rates for the last 36 month-long periods (2048 through 2050); and
- (6) a run for 2000 through 2050 with average recharge rates.

The only change in simulation of normal precipitation versus drought-of-record years was the use of different recharge rates. Pumping rates and their monthly variations were not changed to reflect changes in demand under drought conditions.

Five criteria were used for evaluating the quality of model calibration and verification. First, the difference between simulated and observed water levels was calculated for the steady-state model and end of 1990, as well as for the end of 2000. The number of measured water levels available for comparison were greater for 1990 and 2000 than for the steady-state model. Few data were available for the steady-state calibration, and they occurred in a narrow range near the outcrop with little variation in water-level elevation. Model calibration is measured by three calculated errors: root mean squared error (RMSE), mean absolute error (MAE), and mean error (ME) (Anderson and Woessner, 1992, p. 238-241). The increase in range of measured water levels and the increase in number of measurements result in an improvement in model performance in this model (a decrease in the ratio of RMSE to the range of water levels in the data set), except for layer 6, representing the Hooper aquitard.

The second calibration measure is minimizing the residual differences between simulated and observed water levels. One calibration goal is that the residual should also show no spatial bias.

A third calibration criterion is that the simulated and measured water levels for individual monitoring wells should match through time. We chose monitoring wells with

long-duration records in each layer of the Carrizo–Wilcox aquifer for hydrograph matching. Owing to error inherited from the steady state calibration, however, a simulated hydrograph may parallel the measured hydrograph but be offset by some baseline shift. To compensate for such baseline shift, we calculated the RMSE of hydrographs by

- (1) Estimating the trend of the measured water levels and the trend of simulated water levels through time to exclude anomalous outlier data,
- (2) Determining the baseline shift needed to adjust each simulated hydrograph to minimize the difference with a measured hydrograph, and
- (3) Calculating the RMSE between the measured water level and the shifted value of the simulated water level.

The RMSE and baseline shift are reported on each hydrograph in section 9.1.

The fourth calibration measure is comparison of rates of simulated and observed base-flow discharge to streams. As previously mentioned, stream-flow calibration numbers include results from historical low-flow studies, base-flow separation studies between gaged stations, and base flow unitized for the size of the watershed in the Carrizo–Wilcox outcrop. All base-flow calibration targets do not have the same quality.

A fifth calibration requirement is that the numerical difference in the water budget between inflow and outflow should be less than 1 percent.

Our approach for building the model was to use as much geological and hydrological information as possible. Improving calibration involved a combination of fixing obvious errors in model input, recognizing reported water levels that were invalid or assigned to the wrong aquifer layer, and adjusting those parameters that are not well constrained by data, such as vertical hydraulic conductivity and storativity. We minimized other cell-by-cell adjustments to not “overcalibrate” the model, a stated desire of the GAM models.